# Evolution of SHMR at z=0-7 Identified by Clustering Analysis with the Hubble Legacy Imaging and Early Subaru/HSC Survey Data

Harikane+15, submitted to ApJ, arXiv 1511.07873

Yuichi Harikane (The University of Tokyo),

Masami Ouchi, Yoshiaki Ono, Surhud More, Shun Saito, Yen-Ting Lin, Jean Coupon, Kazuhiro Shimasaku, Takatoshi Shibuya, Paul A. Price, Lihwai Lin, Bau-Ching Hsieh, Masafumi Ishigaki, Yutaka Komiyama, John Silverman, Tadafumi Takata, Hiroko Tamazawa, and Jun Toshikawa

# Outline

- Introduction of stellar-to-halo mass ratio (SHMR)
- HSC & Hubble Data and LBG Selection
- Clustering Analysis with HOD Model
- Results of Halo Mass, SHMR, Com w/ AM
- Discussion: Evolution of SHMR

# Galaxy-Dark Halo Connection: SHMR

- Dark matter halo is a key for galaxy formation.
  - Gas cooling is efficient in $10^{10}$-$10^{13}$ $M_{sun}$ halo (Silk+93).
  - SN/AGN feedback in low/high mass halo (e.g., YH+14).
  - Merger rate is a function of the halo mass (Fakhouri+10).

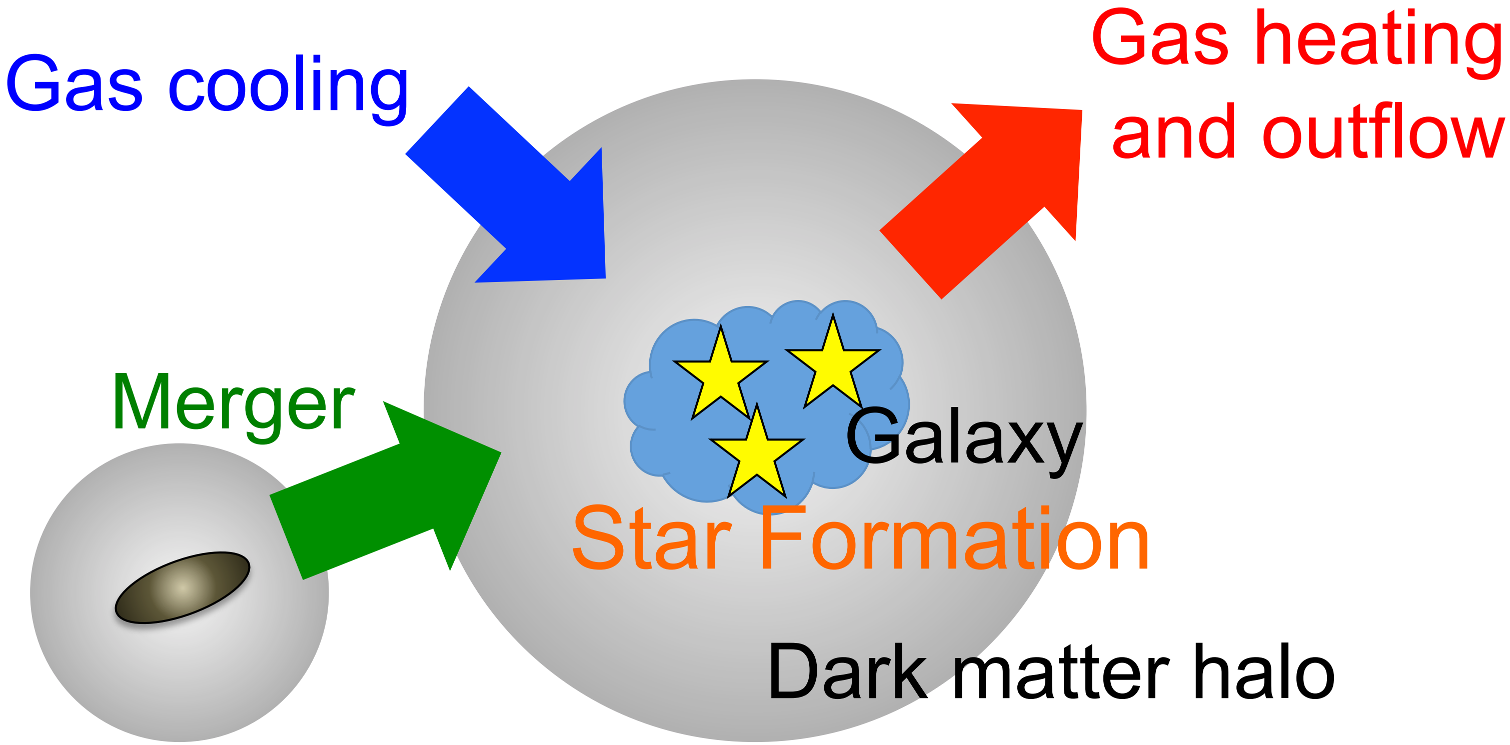

# Stellar-to-halo mass ration (SHMR)

- SHMR=$M_*/M_h$: past star formation efficiency per $M_h$
- SHMR at z>1: not well studied by galaxy clustering
- Abundance matching (AM): SHMR at z=0-8

  -> systematic uncertainty?

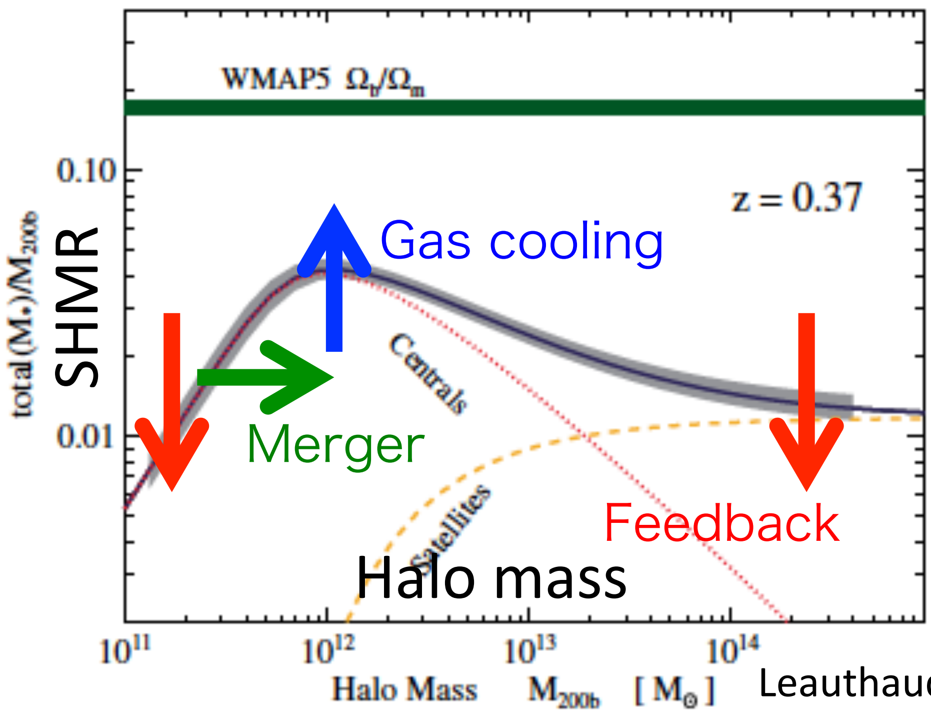


Leauthaud+12

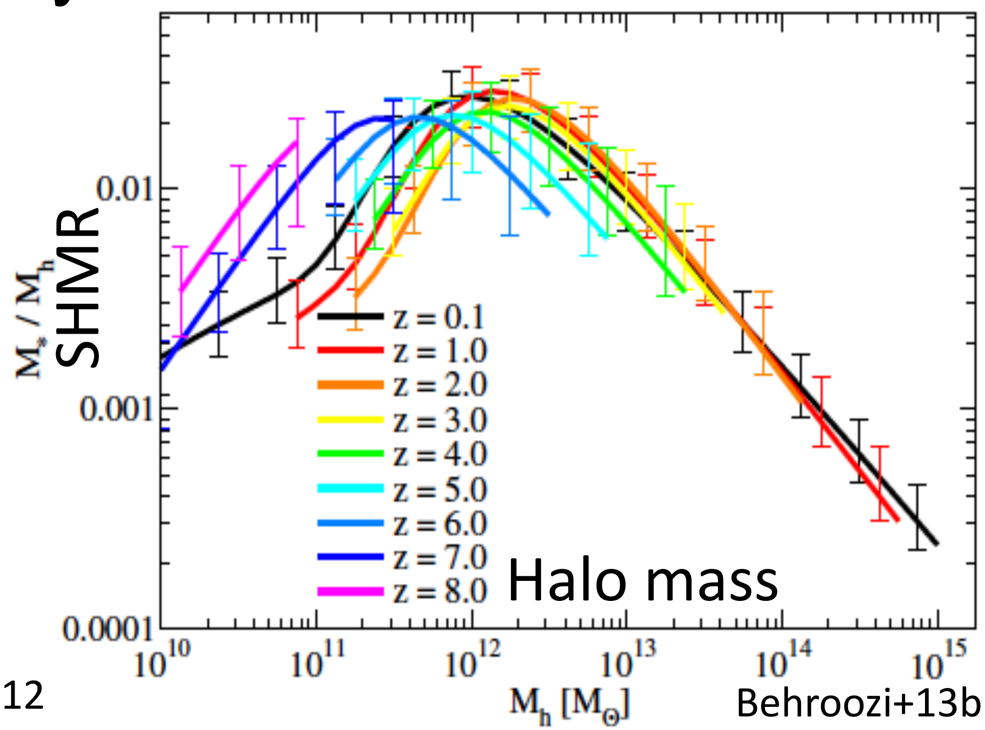


Behroozi+13b

# This Study

Method:

Clustering analysis w/ halo occupation distribution (HOD) model & abundance

+

Data:

Hubble & Subaru/HSC

↓

**SHMR at high-z**

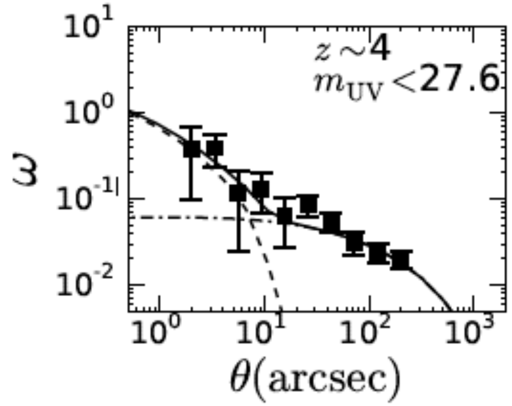


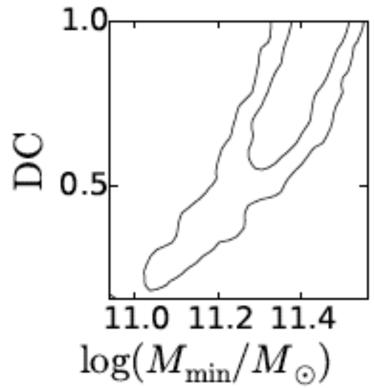


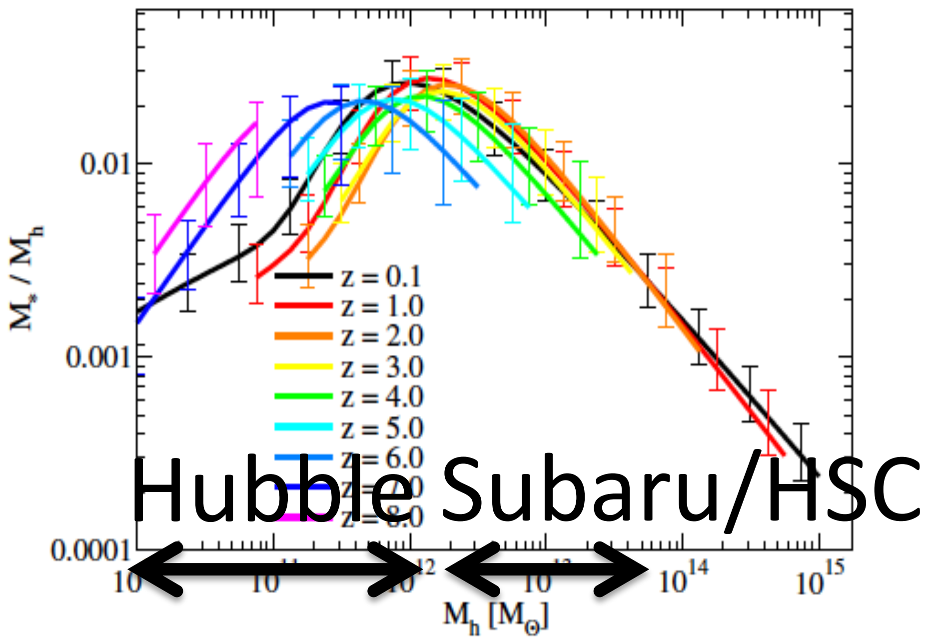

# Data & Sample Selection

Lyman break galaxy (LBG) selection @z~4, 5, 6, 7

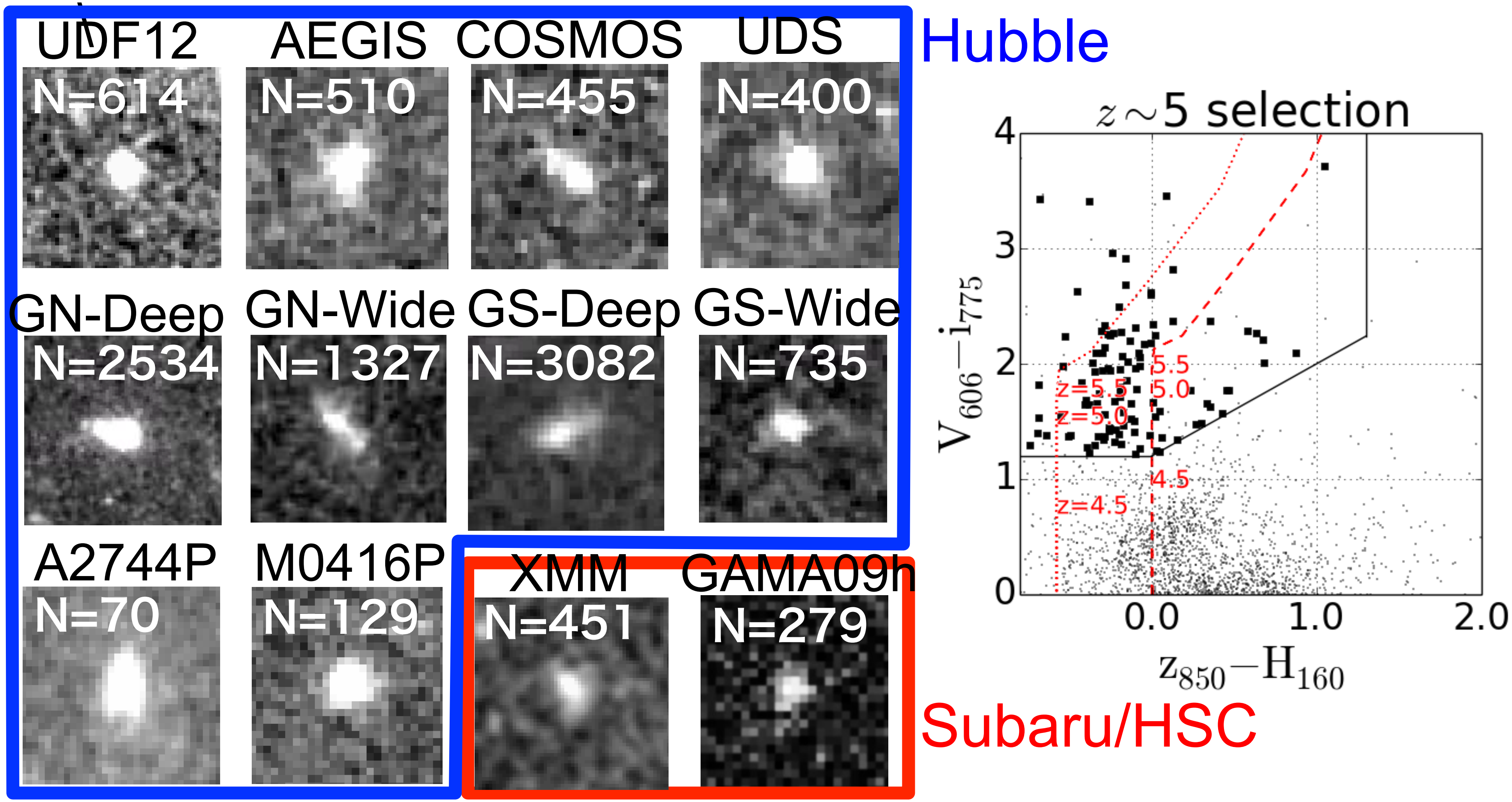


Total of 10540 LBGs at z=4-7

# Clustering Analysis w/ HOD Model

Calculate Angular Correlation Function in Each Subsample

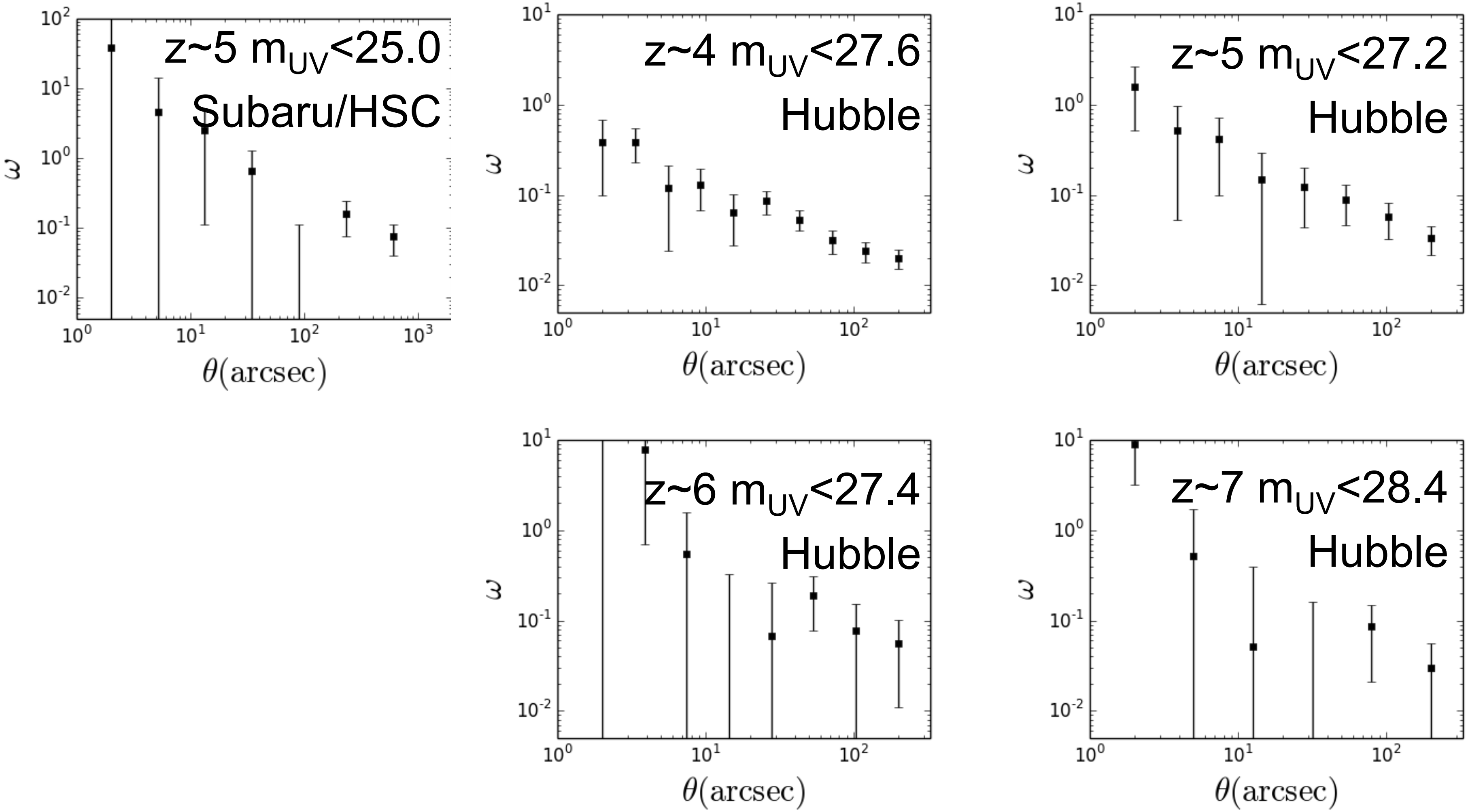

# Clustering Analysis w/ HOD Model

Calculate Angular Correlation Function in Each Subsample

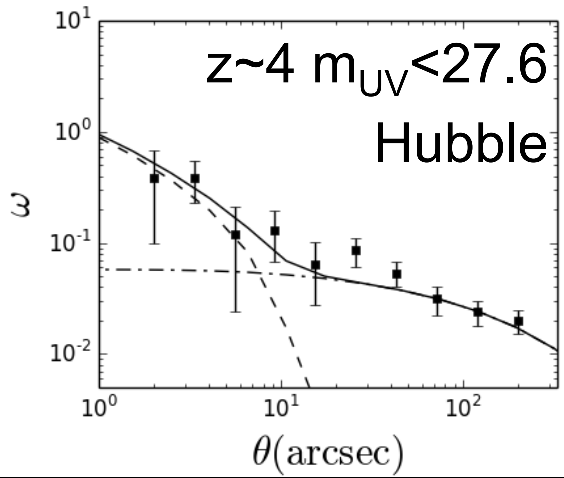


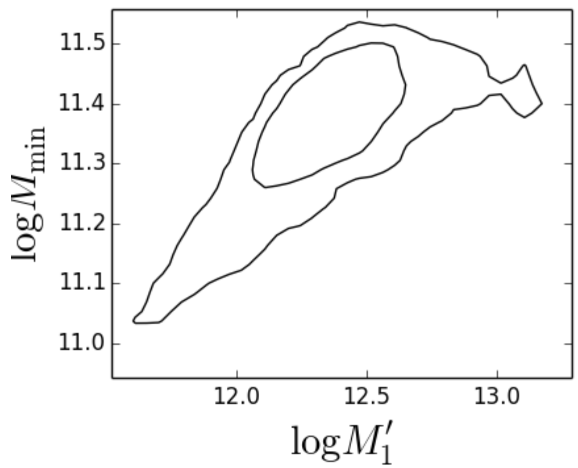


Fit w/ Prediction by the Structure Formation & HOD models

$$P_g^{1h} = \frac{1}{n_g^2}\int dM \left[N_s(M)N_s(M)u^2(k,M) + 2N_s(M)N_c(M)u(k,M)\right]\frac{dn}{dM}(M,z)$$

$$P_g^{2h} = P_m(k,z)\left[\frac{1}{n_g}\int dM N(M)\frac{dn}{dM}(M,z)b_h(M,z)u(k,M)\right]^2$$

Estimate Dark Halo Mass

# Dark Halo Mass

- Hubble: $M_h \sim 10^{10}$-$10^{11}$ $M_{sun}$.
- Subaru/HSC: $M_h > 10^{12}$ $M_{sun}$.

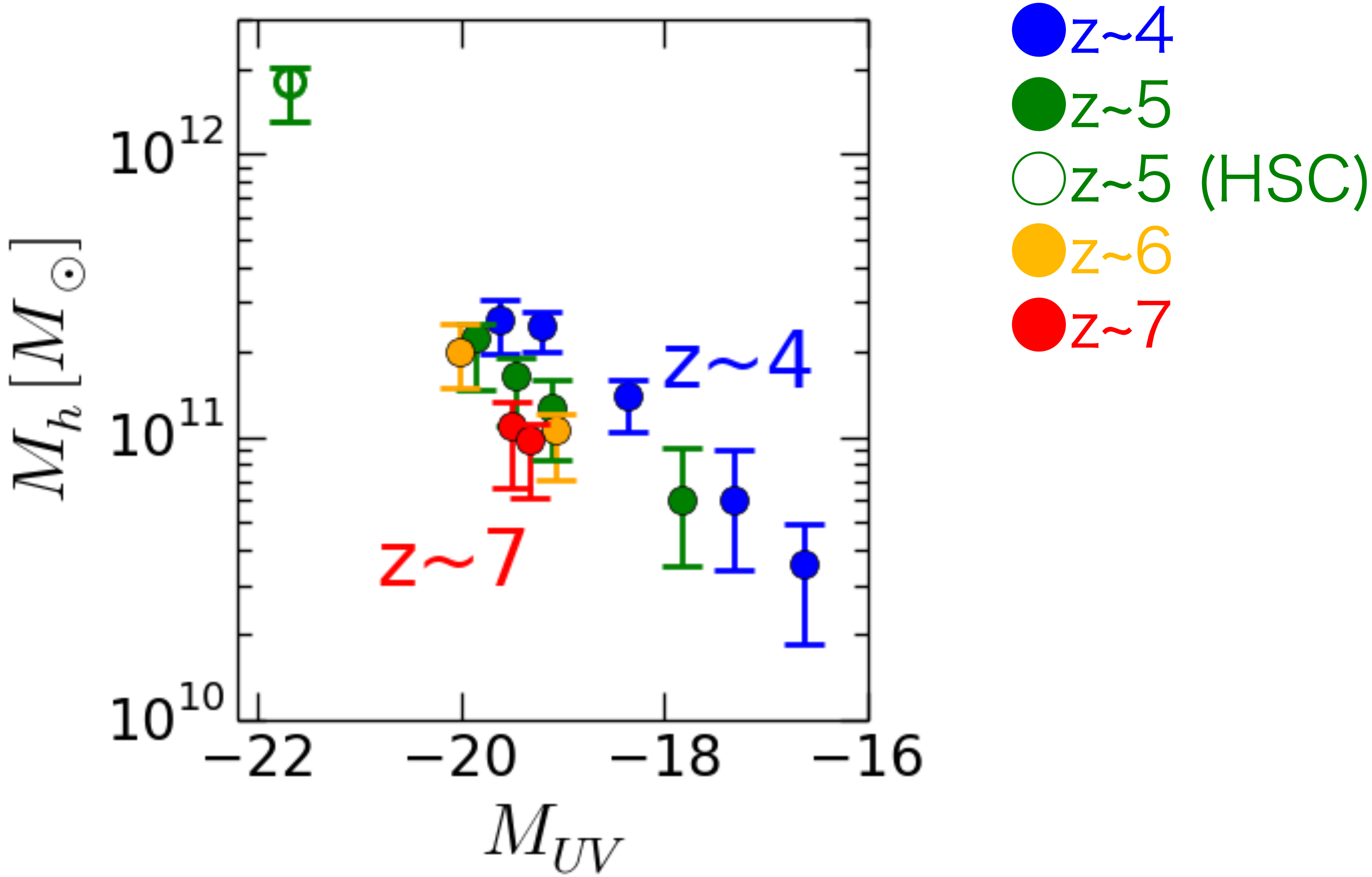

# SHMR

- We estimate SHMR=$M_*/M_h$ at z~4-7

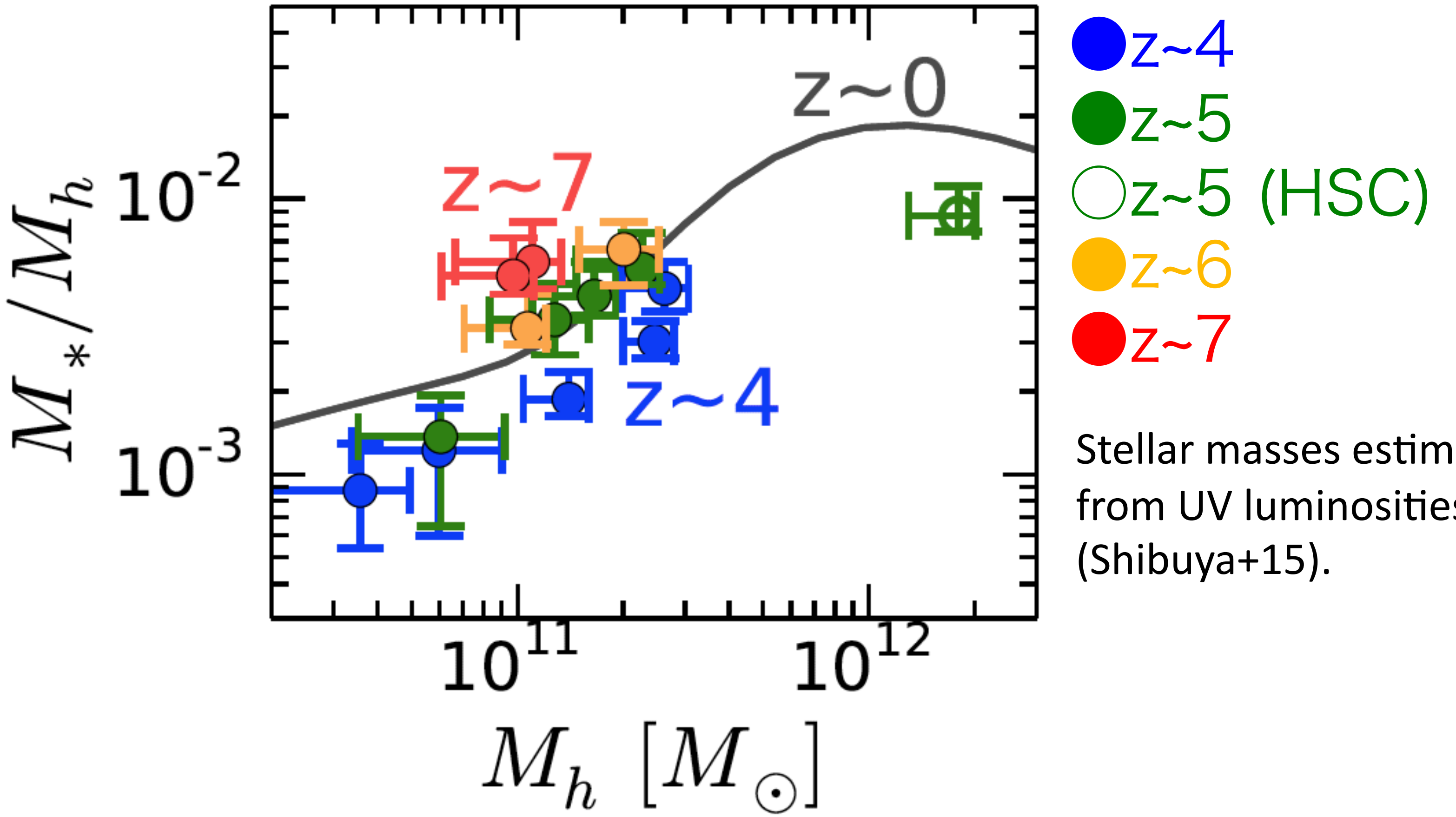


Stellar masses estimated from UV luminosities (Shibuya+15).

# SHMR

- We estimate SHMR=$M_*/M_h$ at z~4-7
- SHMR evolution w/ redshift is found (>98% CL)

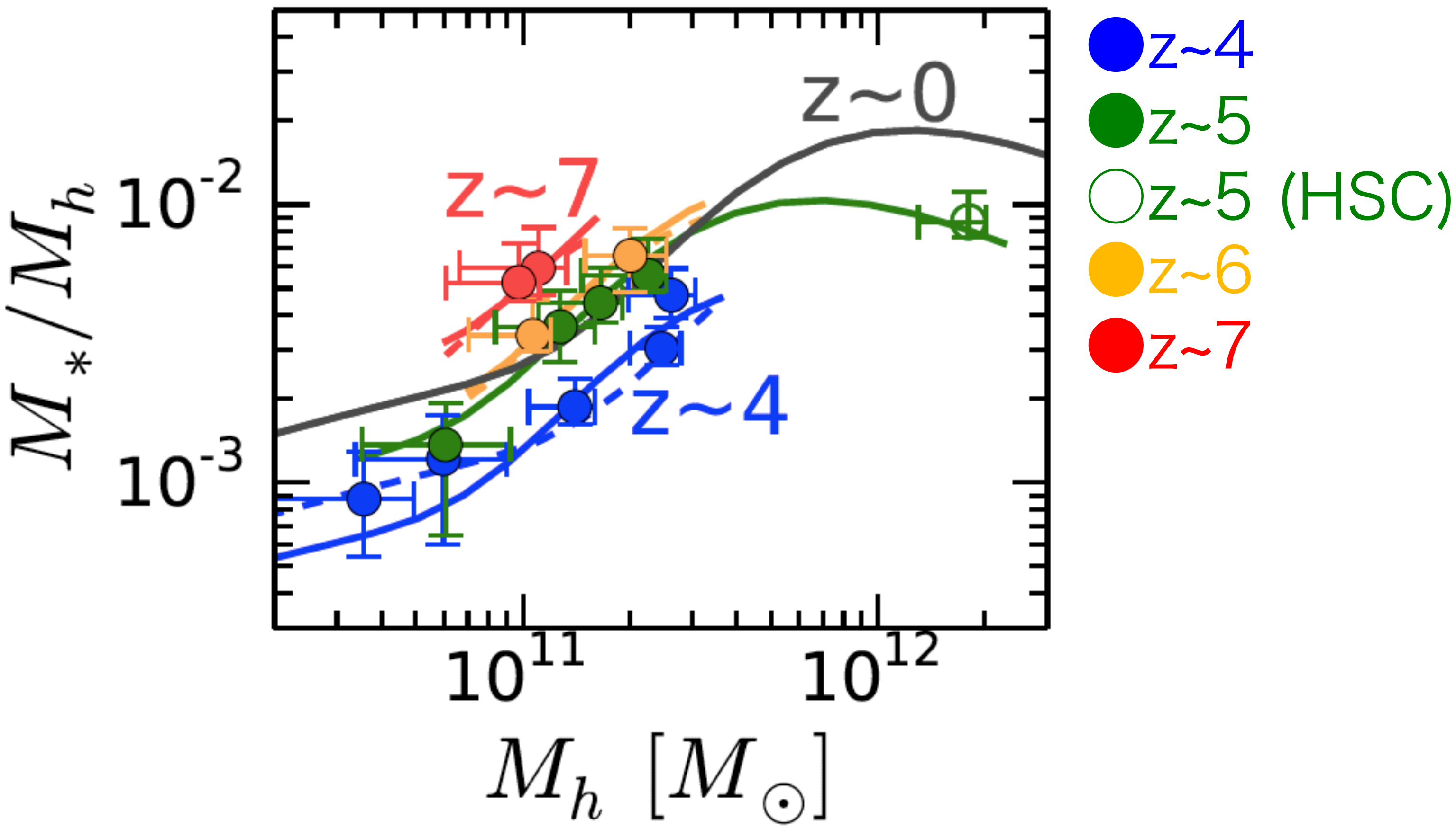

# Comparison with AM

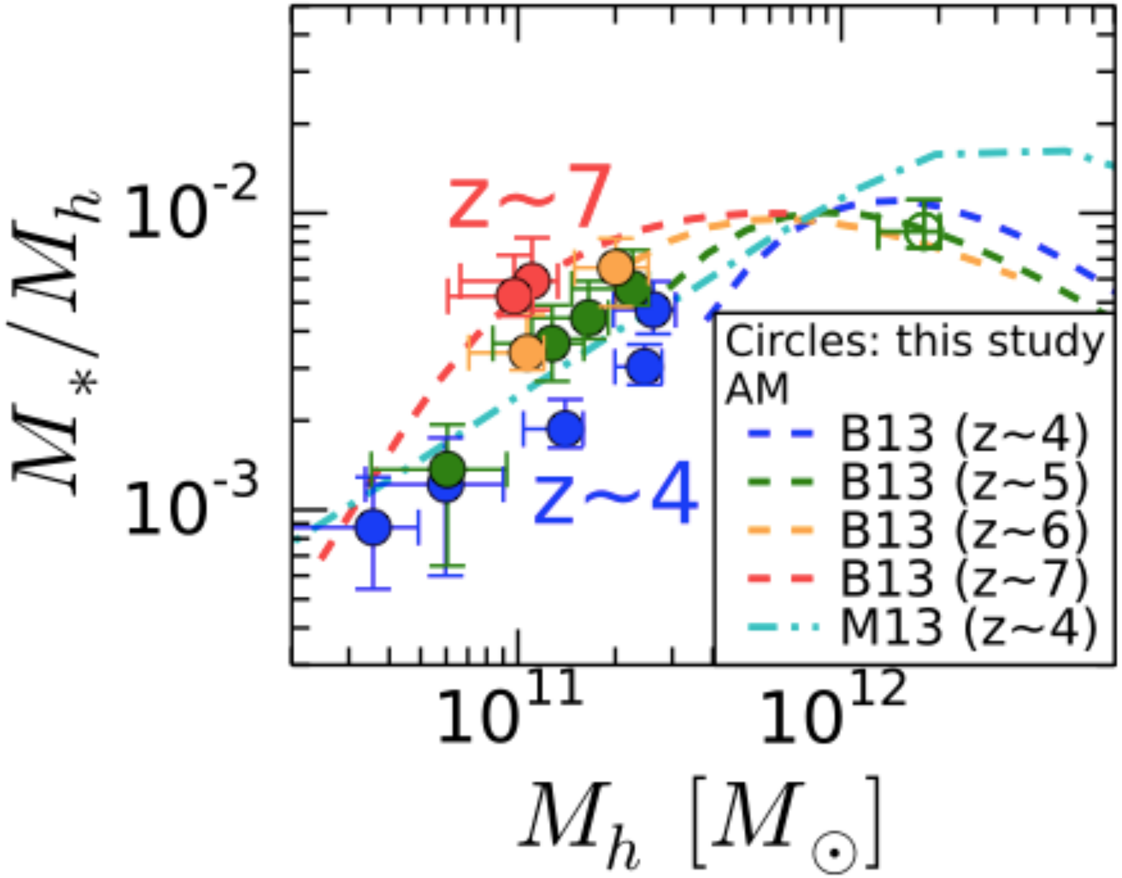


- The difference is up to a factor of ~3 in $M_h$.
  - AM is useful to estimate $M_h$ of high-z galaxy, if one allows the systematic uncertainties up to a factor of 3.

# Discussion: Evolution of SHMR

- SHMR ($M_h = 10^{11}$ $M_{sun}$)
  - Decrease from z~7 to 4, increase from z~4 to 0

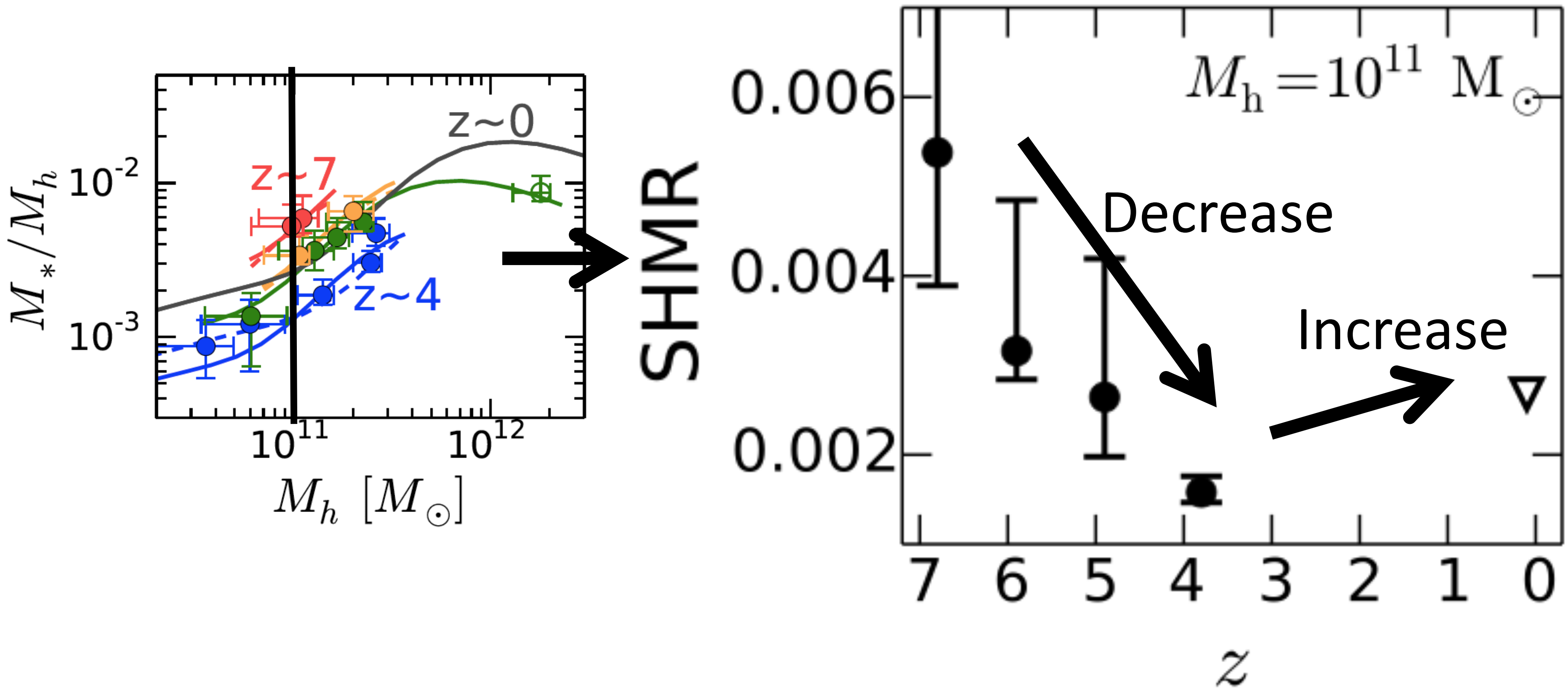

# Comparison with Theoretical Studies

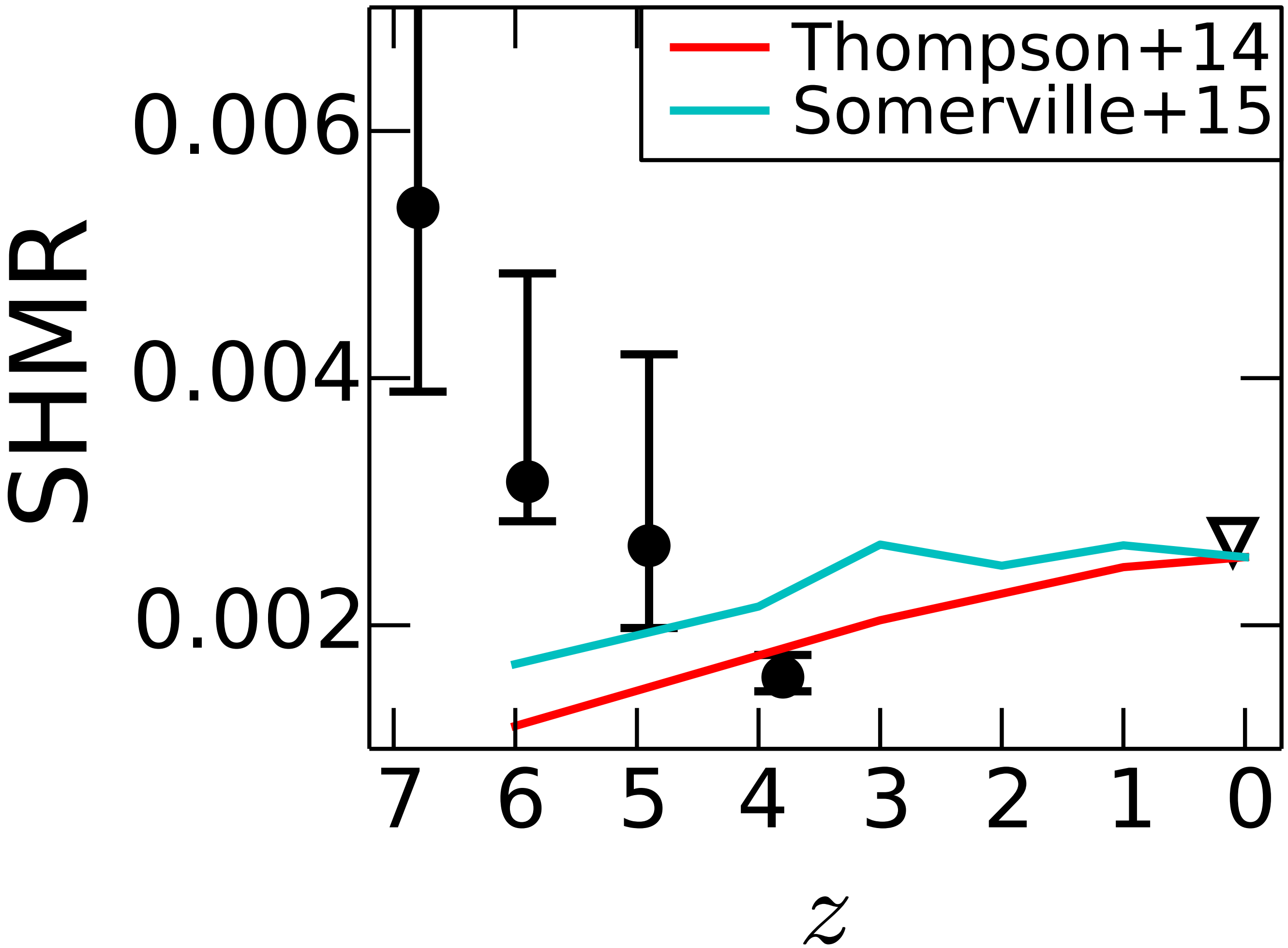


- z~0-4: trend is similar
- z~4-6: inconsistent with our results

# Comparison with standard models

1. Gas cooling model 2. Negative feedback model

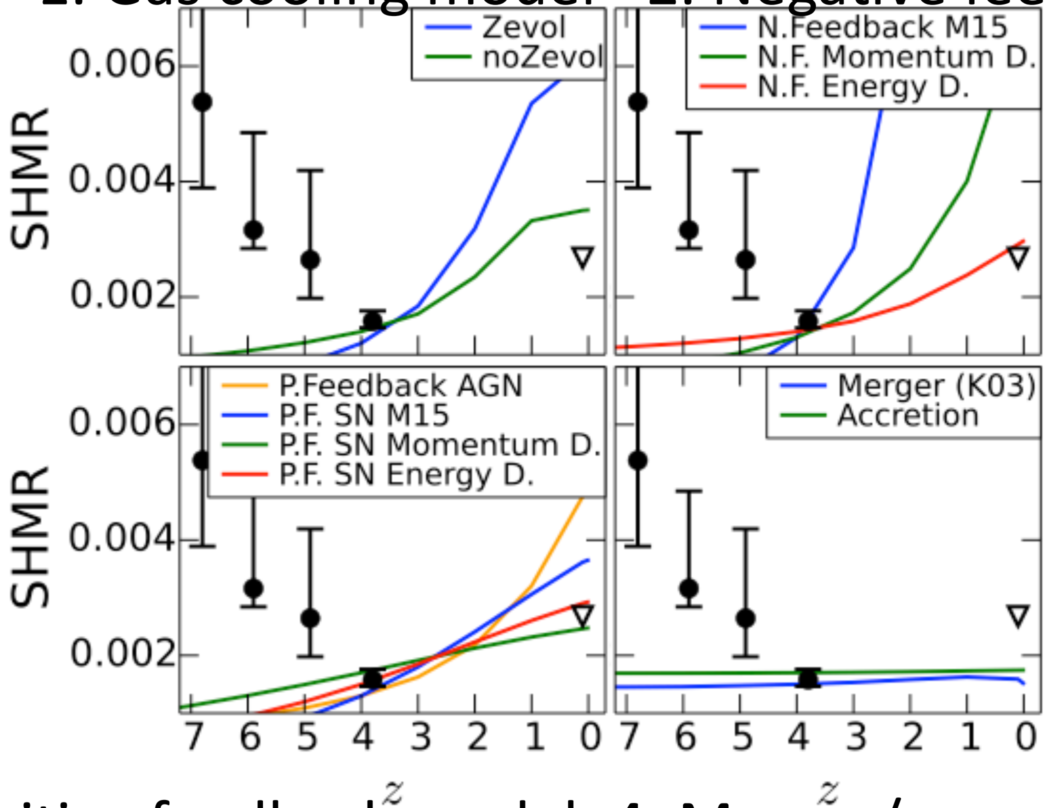


3. Positive feedback model 4. Merger/accretion model

- SHMR increase z~4->0: some model can explain
- SHMR decrease z~7->4: no model can explain

-> Another physical mechanism could be needed.

# Summary

- We select 10540 LBGs with Subaru/HSC and Hubble data.
- SHMR evolution: decrease from z~7 to 4, increase from z~4 to 0 (>98%CL for $M_h$~$10^{11}M_{sun}$)
- The difference between our results and AM results is up to a factor of 3 in $M_h$.
- No model can explain the SHMR evolution at z~4-7
  -> Another physical mechanism could be needed.

# Discussion2 : Baryon Conversion Efficiency

- Baryon conversion efficiency (BCE) =SFR/($dM_b$/dt)
  - Conversion rate from baryonic gas to stars
  - $dM_b/dt = f_b \times dM_h/dt(z, M_h)$ ($f_b = \Omega_b / \Omega_m$)

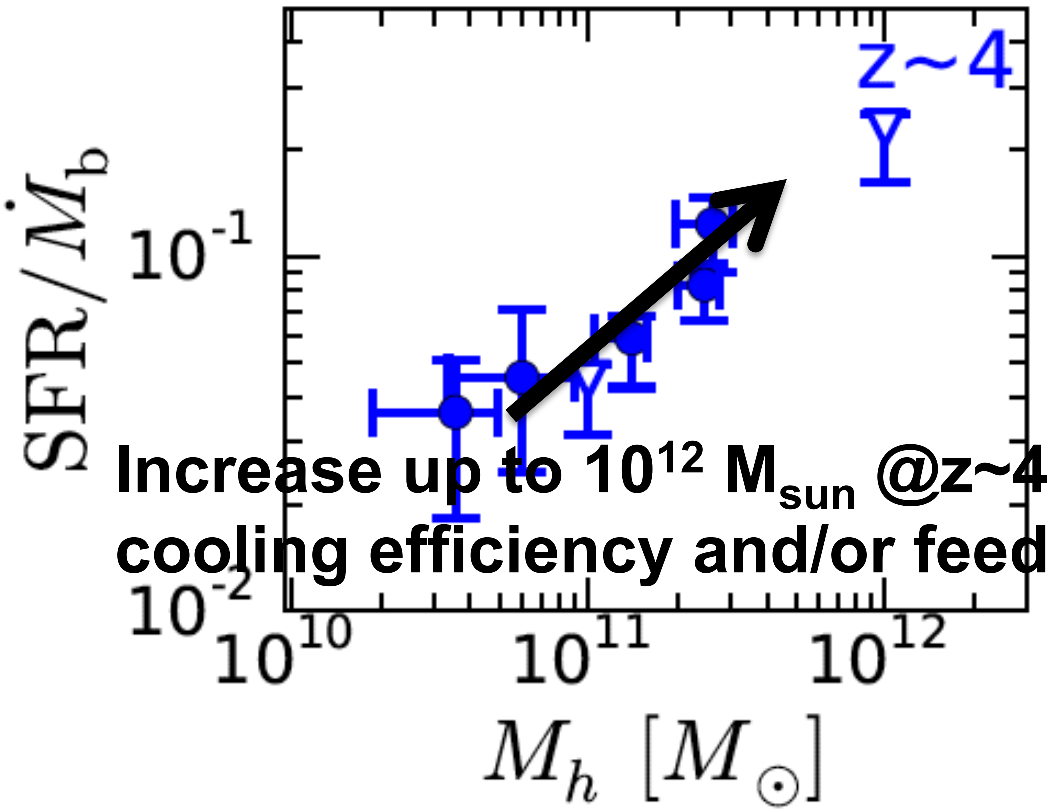


●z~4
▽z~4
(Behroozi+13)

**Increase up to $10^{12}$ $M_{sun}$ @z~4 due to gas cooling efficiency and/or feedback?**

# Discusson3: comparison with AM

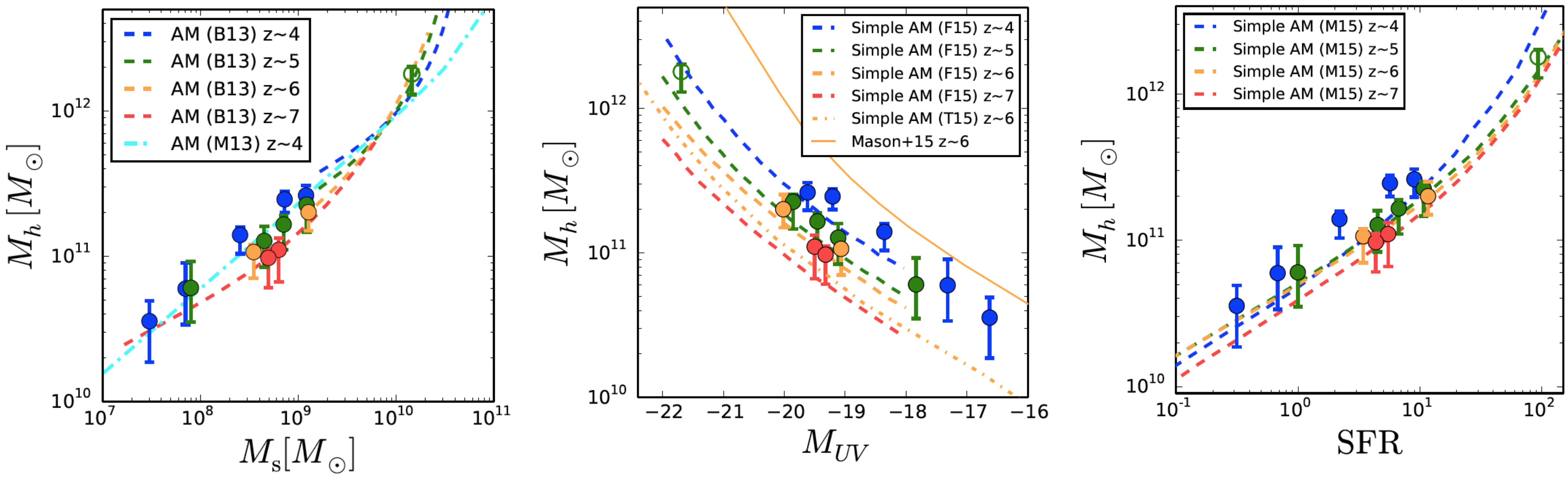


- Difference between our results (clustering+HOD) and AM is up to factor ~3 in $M_h$
- AM is useful to estimate $M_h$ of high-z galaxy halos, if one allows the systematic uncertainties up to a factor of 3.

# Summary

We investigate the galaxy-dark matter halo connection at z~4-7 by clustering analysis with Hubble and Subaru/HSC data.

Main results are

1. SHMR evolution: decrease z~7->4, increase z~4->0
2. BCE: increase w/ increasing dark matter halo mass
3. Com w/ AM: difference is up to factor ~3 in $M_h$

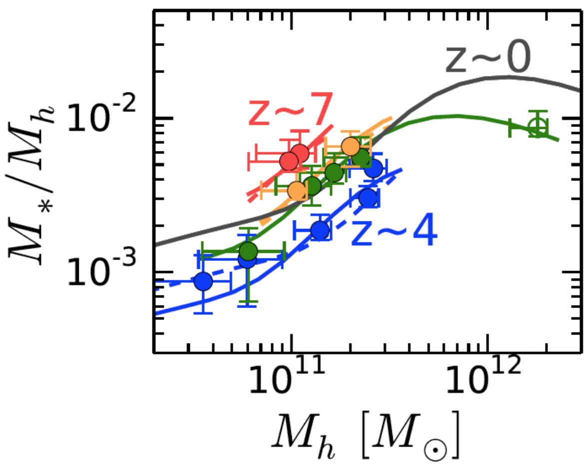


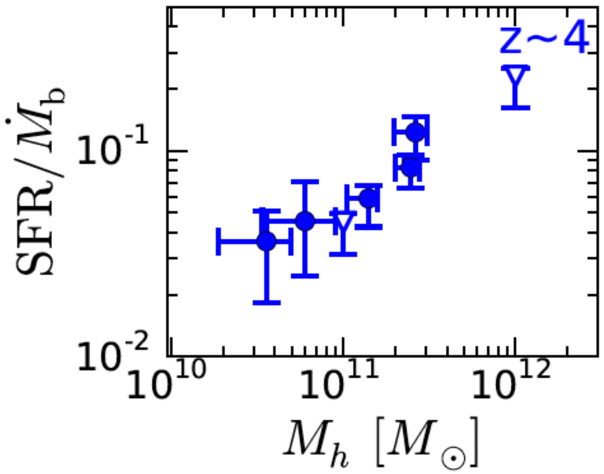


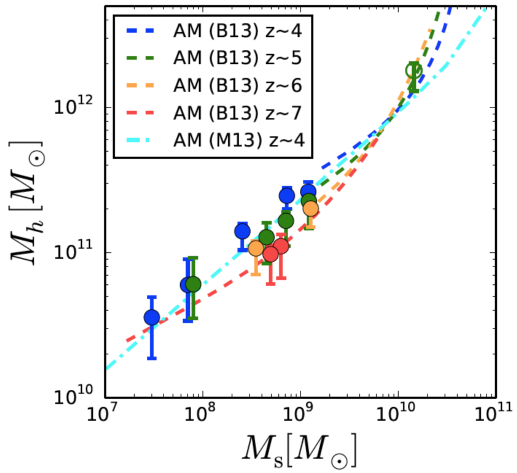

# Results: Dark Halo Mass

- Dark halo mass estimates are consistent with previous HOD results.

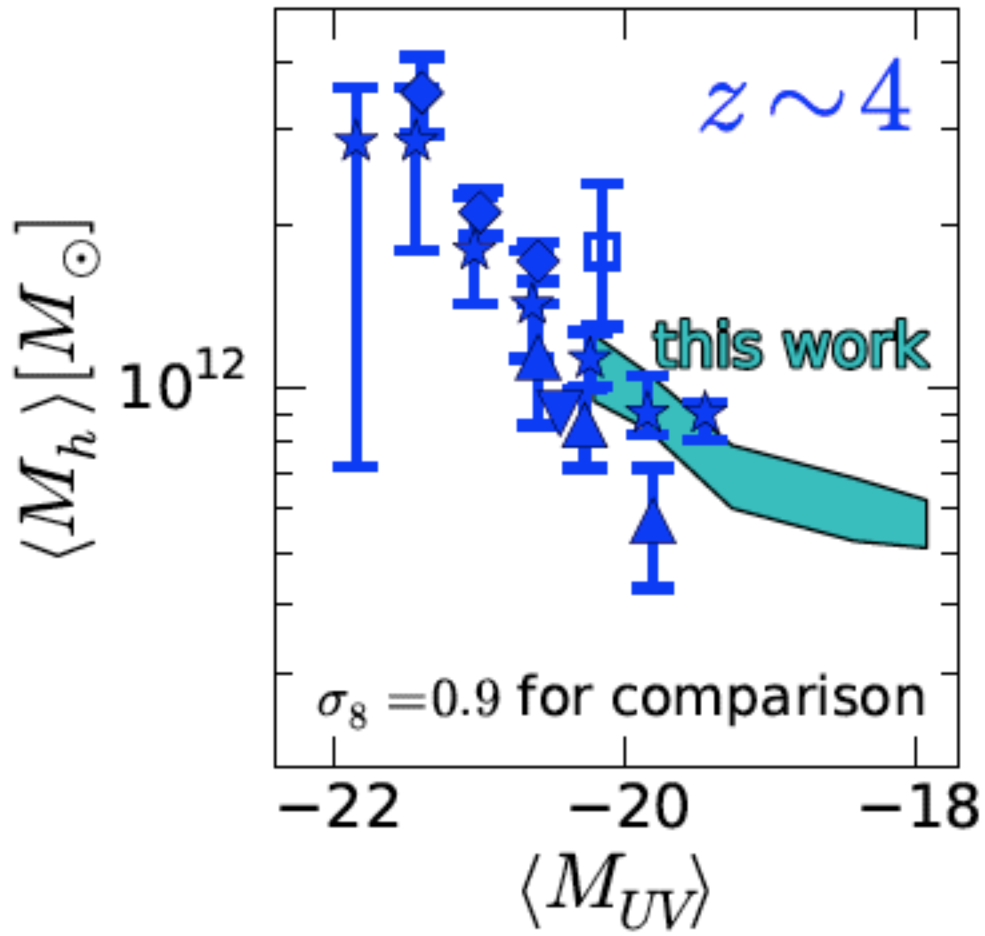

# Details of HOD Model

1 halo term $P_g^{1h} = \frac{1}{n_g^2}\int dM \left[N_s(M)N_s(M)u^2(k,M) + 2N_s(M)N_c(M)u(k,M)\right]\frac{dn}{dM}(M,z)$

2 halo term $P_g^{2h} = P_m(k,z)\left[\frac{1}{n_g}\int dM N(M)\frac{dn}{dM}(M,z)b_h(M,z)u(k,M)\right]^2$

$$N(M) = N_c(M) + N_s(M)$$

$$N_c(M) = \frac{1}{2}DC(M)\left[1 + \mathrm{erf}\left(\frac{\log M - \log M_{\min}}{\sigma_{\log M}}\right)\right]$$

$$N_s(M) = N_c(M)\left(\frac{M - M_0}{M_1'}\right)^\alpha$$

We assume,

- DC(M)=DC (constant)
- $\sigma_{\log M}$=0.2 (fix)
- α=1.0 (fix)
- $\log M_0 = 0.76 * \log M_1' + 2.3$ from Martinez-Manso+15
- ($\log M_1' = 1.18 * \log M_{min} - 1.28$)

Free parameters: $M_{min}$, DC, ($M_1'$)

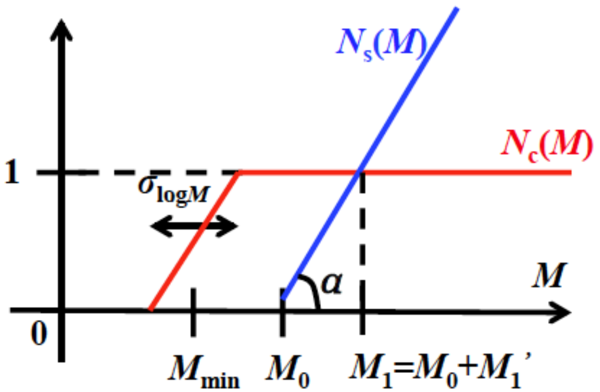


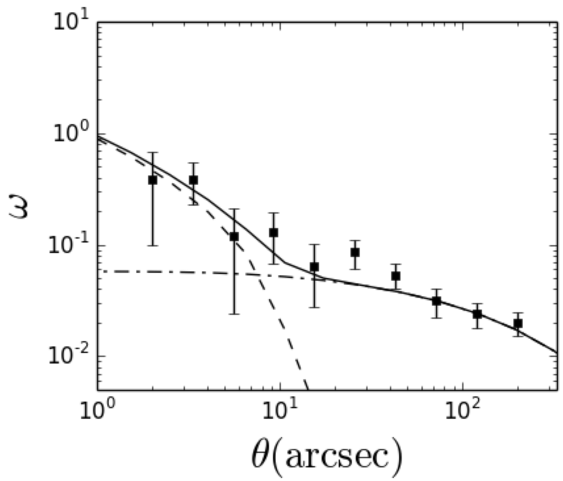


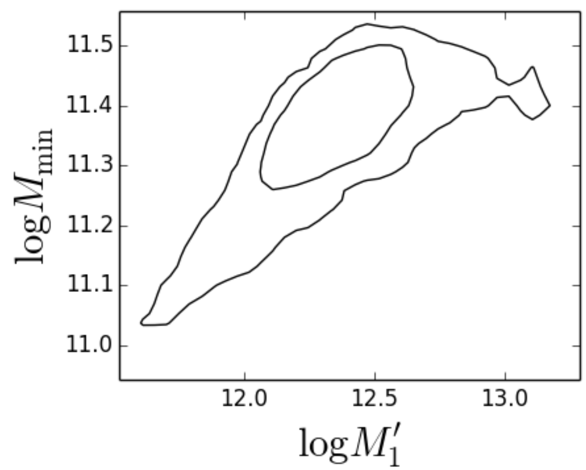

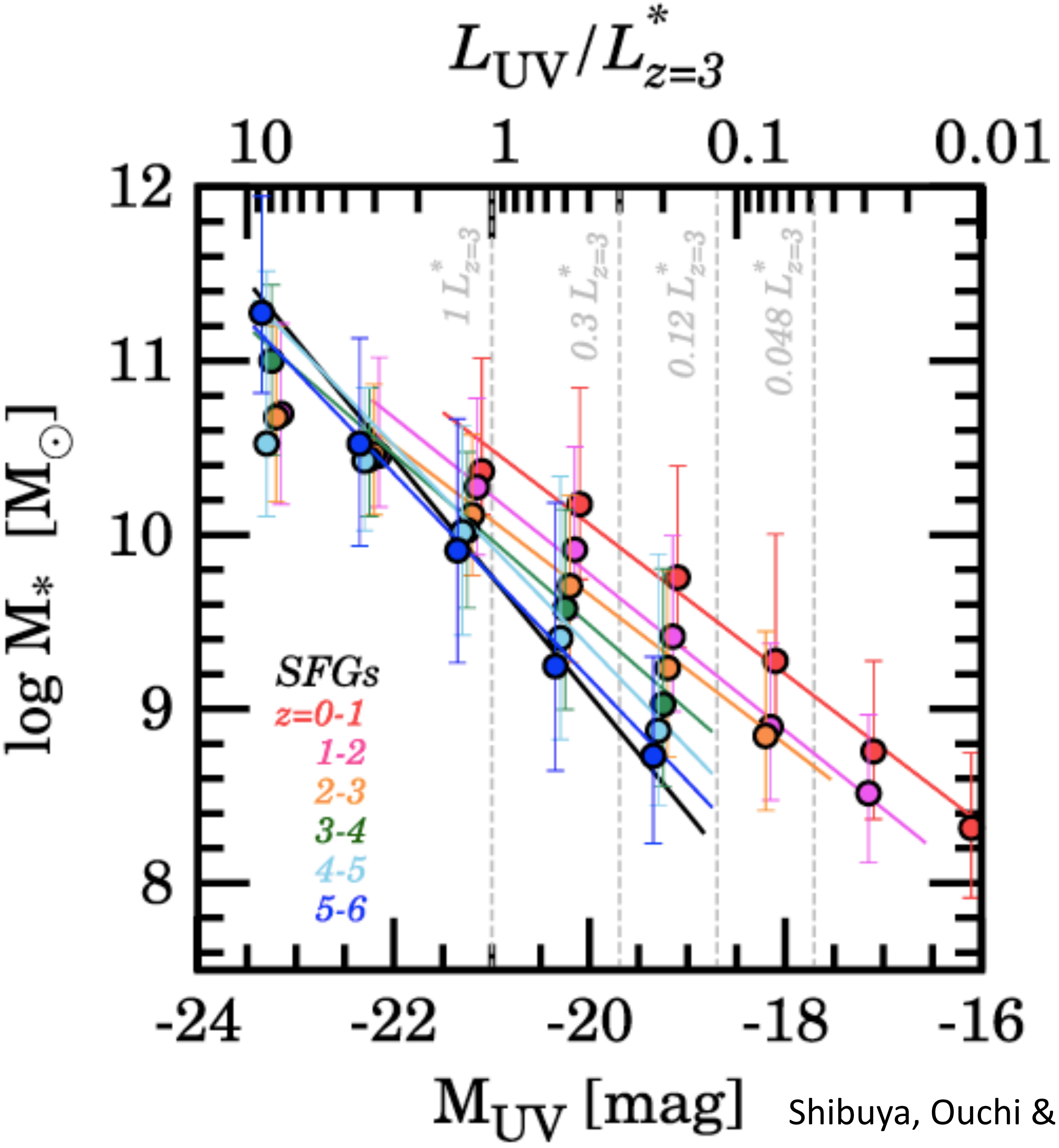


Shibuya, Ouchi & Harikane+15

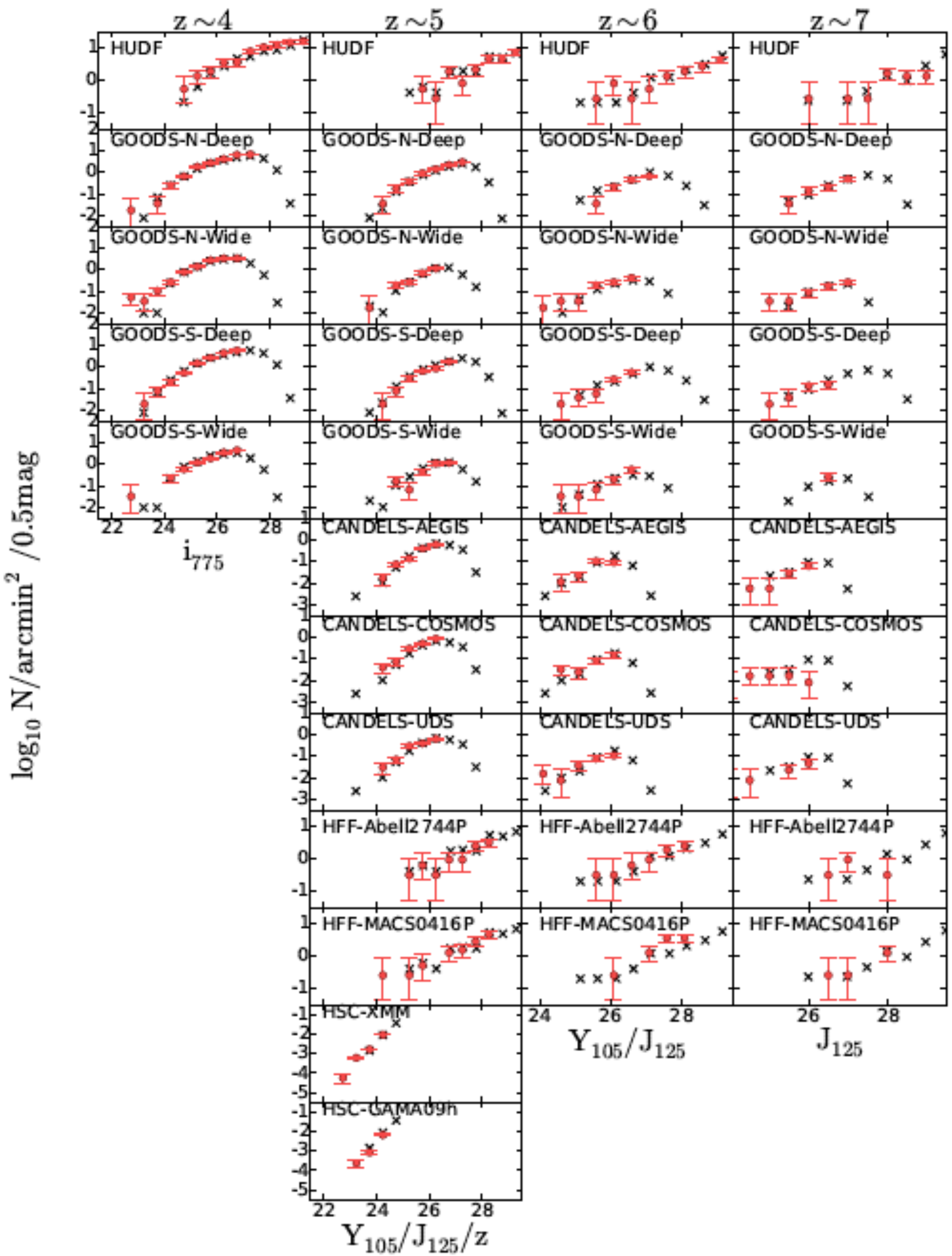

z ∼4
z ∼5
z ∼6
z ∼7
HUDF
GOODS-N-Deep
GOODS-N-Wide
GOODS-S-Deep
GOODS-S-Wide
CANDELS-AEGIS
CANDELS-COSMOS
CANDELS-UDS
HFF-Abell2744P
HFF-MACS0416P
HSC-XMM
HSC-GAMA09h
$\log_{10}$ N/arcmin$^2$ /0.5mag
$i_{775}$
$Y_{105}/J_{125}/z$
$Y_{105}/J_{125}$
$J_{125}$

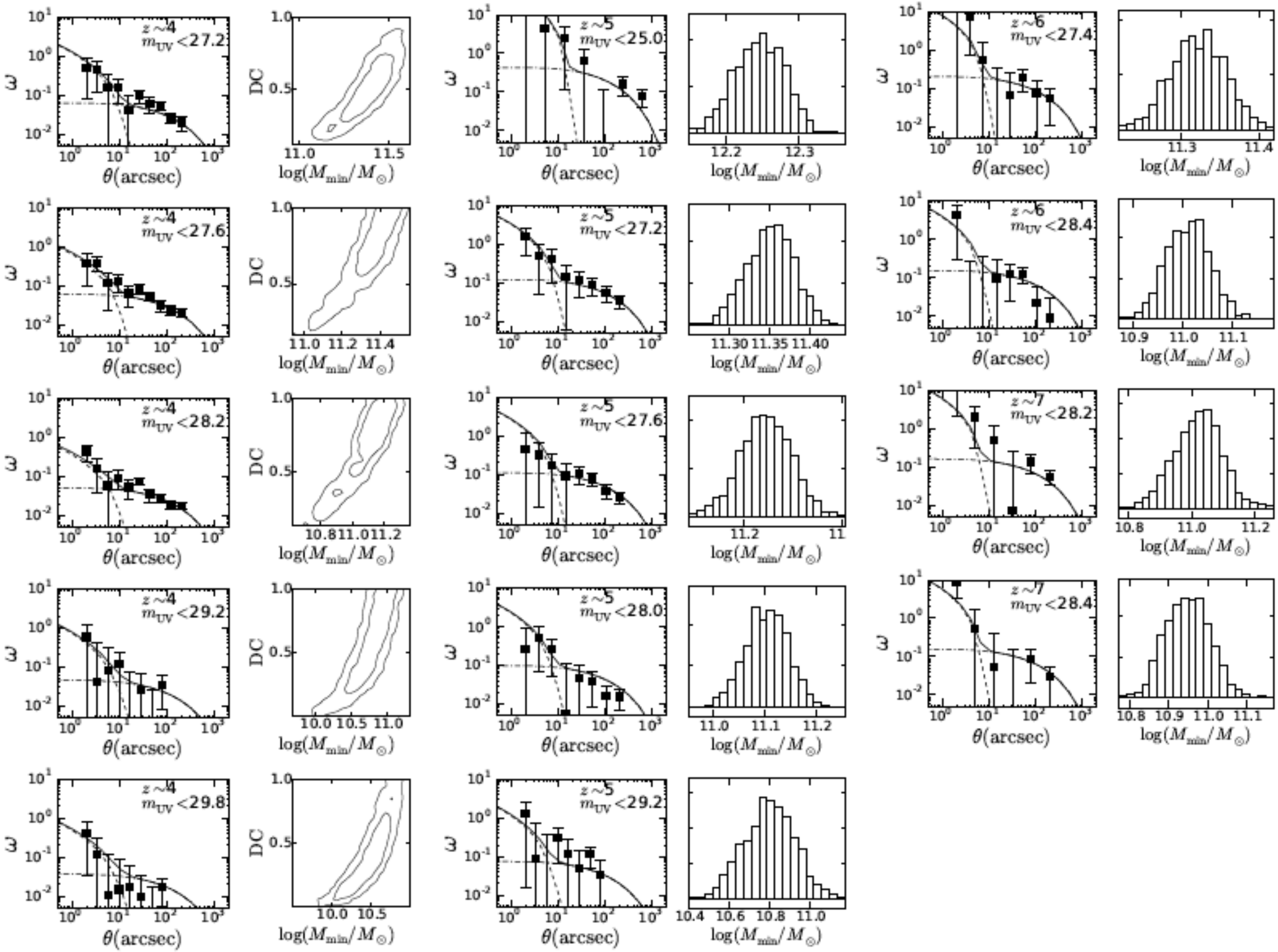

z ~4
m_UV <27.2
m_UV <27.6
m_UV <28.2
m_UV <29.2
m_UV <29.8
z ~5
m_UV <25.0
m_UV <27.2
m_UV <27.6
m_UV <28.0
m_UV <29.2
z ~6
m_UV <27.4
m_UV <28.4
z ~7
m_UV <28.2
m_UV <28.4
ω
θ(arcsec)
DC
log(M_min/M_⊙)

Number of LBGs for our Analysis

| Field (1) | Area ($\mathrm{arcmin}^2$) (2) | $5\sigma$ depth (3) | $z \sim 4$ (4) | $z \sim 5$ (5) | $z \sim 6$ (6) | $z \sim 7$ (7) |
|---|---|---|---|---|---|---|
| HUDF | 3.7 | 30.6 | 290 (348) | 48 (130) | 0 (86) | 0 (50) |
| GOODS-N-Deep | 57.4 | 28.6 | 1411 (1655) | 431 (630) | 43 (136) | 81 (113) |
| GOODS-N-Wide | 58.2 | 28.1 | 788 (800) | 193 (223) | 63 (69) | 27 (235) |
| GOODS-S-Deep | 52.7 | 29.0 | 1139 (1872) | 205 (696) | 142 (311) | 66 (203) |
| GOODS-S-Wide | 30.4 | 28.3 | 461 (510) | 92 (142) | 28 (51) | 13 (31) |
| CANDELS-AEGIS | 174.9 | 28.0 | ... | 304 (381) | 73 (101) | 0 (28) |
| CANDELS-COSMOS | 122.0 | 27.9 | ... | 314 (348) | 76 (80) | 0 (27) |
| CANDELS-UDS | 129.3 | 27.9 | ... | 268 (310) | 54 (65) | 0 (25) |
| HFF-Abell2744P | 3.1 | 29.3 | ... | 30 (37) | 0 (26) | 0 (7) |
| HFF-MACS0416P | 3.8 | 29.5 | ... | 56 (67) | 0 (53) | 0 (9) |
| HSC-XMM | 30100 | 25.1 | ... | 451 (451) | ... | ... |
| HSC-GAMA09h | 24800 | 25.0 | ... | 279 (279) | ... | ... |
| $N_{\mathrm{total}}(z)$ | | | 4089 (5185) | 2671 (3694) | 585 (978) | 291 (728) |
| $N_{\mathrm{total}}$ | | | | 7636 (10703) | | |

**Note**. — Columns: (1) Field. (2) Effective area in $\mathrm{arcmin}^2$. (3) $5\sigma$ limiting magnitude in coadd image )-(7) Number of the LBGs for our analysis at each redshift that are brighter than $5\sigma$ limiting magnitud rest-frame UV band. The parentheses represent the number of LBGs in the parent sample.

| $z_c$ | $m_{\mathrm{UV,th}}$ | $M_{\mathrm{UV,th}}$ | $\langle M_{\mathrm{UV}} \rangle$ | $\log\mathrm{SFR}_{\mathrm{th}}$ | $\log M_{*,\mathrm{th}}$ | $N$ | $n_{\mathrm{g}}$ ($10^{-4}$ Mpc$^{-3}$) | $A_\omega$ (arcsec$^{0.8}$) | $r_0$ (Mpc) | $b_{\mathrm{g}}$ | $\chi^2_\nu$ |
|---|---|---|---|---|---|---|---|---|---|---|---|
| (1) | (2) | (3) | (4) | (5) | (6) | (7) | (8) | (9) | (10) | (11) | (12) |
| 3.8 | 27.2 | -19.6 | -20.2 | 0.97 | 9.1 | 1406 | $20.1 \pm 3.5$ | $1.2 \pm 0.2$ | $5.7^{+0.4}_{-0.4}$ | $2.9^{+0.2}_{-0.2}$ | 0.6 |
| | 27.6 | -19.2 | -19.8 | 0.77 | 8.9 | 2301 | $31.3 \pm 4.9$ | $1.0 \pm 0.1$ | $5.1^{+0.3}_{-0.3}$ | $2.6^{+0.1}_{-0.1}$ | 0.8 |
| | 28.2 | -18.4 | -19.3 | 0.35 | 8.4 | 2509 | $68.6 \pm 11.7$ | $0.8 \pm 0.1$ | $4.4^{+0.2}_{-0.2}$ | $2.4^{+0.1}_{-0.1}$ | 1.4 |
| | 29.2 | -17.3 | -18.4 | -0.15 | 7.9 | 161 | $154.7 \pm 53.8$ | $0.4 \pm 0.3$ | $3.0^{+1.0}_{-1.5}$ | $1.7^{+0.5}_{-0.8}$ | 0.4 |
| | 29.8 | -16.7 | -17.9 | -0.49 | 7.5 | 244 | $251.6 \pm 65.6$ | $0.2 \pm 0.1$ | $2.2^{+0.8}_{-1.0}$ | $1.2^{+0.4}_{-0.5}$ | 0.3 |
| 4.8 | 25.0 | -21.7 | -22.1 | 2.0 | 10.2 | 730 | $0.15 \pm 0.10$ | $8.8 \pm 3.4$ | $14.5^{+2.9}_{-3.5}$ | $8.2^{+1.5}_{-1.8}$ | 0.9 |
| 4.9 | 27.2 | -19.9 | -20.5 | 1.0 | 9.1 | 878 | $9.4 \pm 1.3$ | $2.0 \pm 0.4$ | $6.4^{+0.7}_{-0.7}$ | $4.0^{+0.4}_{-0.4}$ | 0.2 |
| | 27.6 | -19.5 | -20.0 | 0.84 | 8.9 | 1467 | $15.2 \pm 1.7$ | $1.4 \pm 0.3$ | $5.2^{+0.5}_{-0.6}$ | $3.3^{+0.3}_{-0.3}$ | 0.4 |
| | 28.0 | -19.1 | -19.8 | 0.67 | 8.7 | 623 | $22.0 \pm 3.5$ | $0.8 \pm 0.3$ | $3.8^{+0.7}_{-0.8}$ | $2.5^{+0.4}_{-0.5}$ | 0.3 |
| | 29.2 | -17.9 | -18.7 | 0.011 | 7.9 | 120 | $72.7 \pm 30.4$ | $1.2 \pm 0.6$ | $4.9^{+1.1}_{-1.4}$ | $3.1^{+0.6}_{-0.8}$ | 0.4 |
| 5.9 | 27.4 | -20.0 | -20.5 | 1.1 | 9.1 | 285 | $3.8 \pm 0.6$ | $2.7 \pm 1.3$ | $6.4^{+1.5}_{-1.9}$ | $4.7^{+1.0}_{-1.3}$ | 0.6 |
| | 28.4 | -19.1 | -19.3 | 0.55 | 8.6 | 278 | $13.4 \pm 2.5$ | $1.1 \pm 0.7$ | $3.9^{+1.2}_{-1.6}$ | $3.0^{+0.8}_{-1.2}$ | 0.6 |
| 6.8 | 28.2 | -19.5 | -19.9 | 0.75 | 8.8 | 113 | $7.0 \pm 2.5$ | $4.0 \pm 1.2$ | $8.7^{+1.4}_{-1.6}$ | $7.1^{+1.0}_{-1.2}$ | 0.6 |
| | 28.4 | -19.3 | -19.8 | 0.65 | 8.7 | 150 | $9.0 \pm 2.2$ | $1.8 \pm 1.0$ | $5.5^{+1.6}_{-2.2}$ | $4.7^{+1.2}_{-1.7}$ | 0.7 |

| $z_c$ (1) | $m_{\rm UV,th}$ (2) | $\log M_{\rm min}$ (3) | $DC$ (4) | $\log M_1'$ (5) | $b_g^{\rm eff}$ (6) | $\log \langle M_{\rm h} \rangle$ (7) | $\chi_\nu^2$ (8) |
|---|---|---|---|---|---|---|---|
| 3.8 | 27.2 | $11.4^{+0.1}_{-0.1}$ | $0.5^{+0.2}_{-0.2}$ | $(12.2^{+0.1}_{-0.1})$ | $3.6^{+0.1}_{-0.2}$ | $11.9^{+0.0}_{-0.1}$ | 0.9 |
| | 27.6 | $11.4^{+0.1}_{-0.1}$ | $1.0^{+0.0}_{-0.3}$ | $12.4^{+0.2}_{-0.2}$ | $3.5^{+0.1}_{-0.1}$ | $11.8^{+0.0}_{-0.1}$ | 0.8 |
| | 28.2 | $11.1^{+0.1}_{-0.1}$ | $0.8^{+0.1}_{-0.3}$ | $12.1^{+0.2}_{-0.3}$ | $3.1^{+0.1}_{-0.1}$ | $11.7^{+0.0}_{-0.1}$ | 1.1 |
| | 29.2 | $10.8^{+0.2}_{-0.2}$ | $1.0^{+0.0}_{-0.5}$ | $(11.6^{+0.1}_{-0.3})$ | $2.8^{+0.2}_{-0.2}$ | $11.6^{+0.1}_{-0.1}$ | 0.8 |
| | 29.8 | $10.6^{+0.1}_{-0.3}$ | $0.3^{+0.3}_{-0.1}$ | $(11.2^{+0.2}_{-0.3})$ | $2.6^{+0.1}_{-0.1}$ | $11.5^{+0.0}_{-0.1}$ | 1.3 |
| 4.8 | 25.0 | $12.3^{+0.0}_{-0.1}$ | 0.6 (fix) | $(13.2^{+0.1}_{-0.2})$ | $7.6^{+0.3}_{-0.7}$ | $12.4^{+0.0}_{-0.1}$ | 1.6 |
| 4.9 | 27.2 | $11.4^{+0.0}_{-0.2}$ | 0.6 (fix) | $(12.1^{+0.2}_{-0.2})$ | $5.0^{+0.1}_{-0.7}$ | $11.7^{+0.0}_{-0.2}$ | 0.3 |
| | 27.6 | $11.2^{+0.1}_{-0.2}$ | 0.6 (fix) | $(12.0^{+0.1}_{-0.2})$ | $4.7^{+0.2}_{-0.4}$ | $11.6^{+0.1}_{-0.1}$ | 0.9 |
| | 28.0 | $11.1^{+0.1}_{-0.2}$ | 0.6 (fix) | $(11.8^{+0.1}_{-0.2})$ | $4.4^{+0.2}_{-0.3}$ | $11.5^{+0.1}_{-0.1}$ | 1.8 |
| | 29.2 | $10.8^{+0.2}_{-0.2}$ | 0.6 (fix) | $(11.5^{+0.2}_{-0.3})$ | $3.8^{+0.3}_{-0.3}$ | $11.3^{+0.1}_{-0.1}$ | 0.5 |
| 5.9 | 27.4 | $11.3^{+0.1}_{-0.1}$ | 0.6 (fix) | $(12.1^{+0.1}_{-0.2})$ | $6.3^{+0.4}_{-0.4}$ | $11.5^{+0.1}_{-0.1}$ | 0.5 |
| | 28.4 | $11.0^{+0.1}_{-0.2}$ | 0.6 (fix) | $(11.7^{+0.1}_{-0.2})$ | $5.5^{+0.2}_{-0.4}$ | $11.3^{+0.1}_{-0.1}$ | 1.4 |
| 6.8 | 28.2 | $11.0^{+0.1}_{-0.2}$ | 0.6 (fix) | $(11.8^{+0.1}_{-0.3})$ | $6.8^{+0.2}_{-0.8}$ | $11.3^{+0.0}_{-0.2}$ | 0.9 |
| | 28.4 | $11.0^{+0.1}_{-0.2}$ | 0.6 (fix) | $(11.7^{+0.1}_{-0.3})$ | $6.3^{+0.4}_{-0.4}$ | $11.2^{+0.1}_{-0.1}$ | 0.6 |

# HODモデル詳細

$$\omega(\theta) = \int dz N^2(z) \left(\frac{dr}{dz}\right)^{-1} \int dk \frac{k}{2\pi} P_{\rm g}(k,z) J_0[r(z)\theta k],$$

$$P_{\rm g}^{\rm cs}(k,z) = \frac{2}{n_{\rm g}^2} \int dM_{\rm h} \langle N_{\rm c} N_{\rm s} \rangle (M_{\rm h}) \frac{dn}{dM_{\rm h}}(M_{\rm h},z) u(k,M_{\rm h},z)$$

$$P_{\rm g}^{\rm ss}(k,z) = \frac{1}{n_{\rm g}^2} \int dM_{\rm h} \langle N_{\rm s}(N_{\rm s}-1) \rangle (M_{\rm h}) \frac{dn}{dM_{\rm h}}(M_{\rm h},z) u^2(k,M_{\rm h},z),$$

$$P_{\rm g}^{\rm 2h}(k,z) = P_{\rm m}(k,z) \left[\frac{1}{n_{\rm g}} \int dM_{\rm h}\ N(M_{\rm h}) \frac{dn}{dM_{\rm h}}(M,z) b_{\rm h}(M_{\rm h},z) u(k,M_{\rm h},z)\right]^2$$

$$N_{\rm c}(M_{\rm h}) = \frac{1}{2}\left[1 + {\rm erf}\left(\frac{\log M_{\rm h} - \log M_{\rm min}}{\sigma_{\log M}}\right)\right]$$

$$N_{\rm s}(M_{\rm h}) = N_{\rm c}(M_{\rm h}) \left(\frac{M_{\rm h} - M_0}{M_1'}\right)^{\alpha}$$

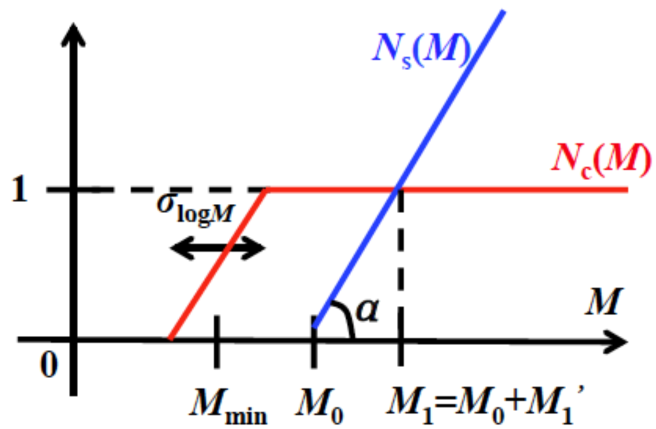

# HODモデル詳細

$$\langle N_c N_s \rangle (M_h) = N_c(M_h) N_s(M_h),$$
$$\langle N_s(N_s - 1) \rangle (M_h) = N_s^2(M_h).$$

- ハロー質量関数 (Behroozi+13, Tinker+08)

$$\frac{dn(M,z)}{dM} = \frac{\overline{\rho}_m}{M} f(\nu)\, d\nu,$$

$$f(\nu) = \alpha[1 + (\beta\nu)^{-2\phi}]\nu^{2\eta} e^{-\gamma\nu^2/2}.$$

- Bias factor (Tinker+10)

$$b(\nu) = 1 - A\frac{\nu^a}{\nu^a + \delta_c^a} + B\nu^b + C\nu^c$$

$$\nu \equiv \delta_c/[D(z)\sigma(M)],$$

- Concentration parameter (Shimizu+03, Bullock+01)

$$c_B(M_{\rm vir},\ z) = \frac{c_{\rm norm}}{1+z}\left(\frac{M_{\rm vir}}{1.4 \times 10^{14}\ h_{70}^{-1}\ M_\odot}\right)^{-0.13}$$

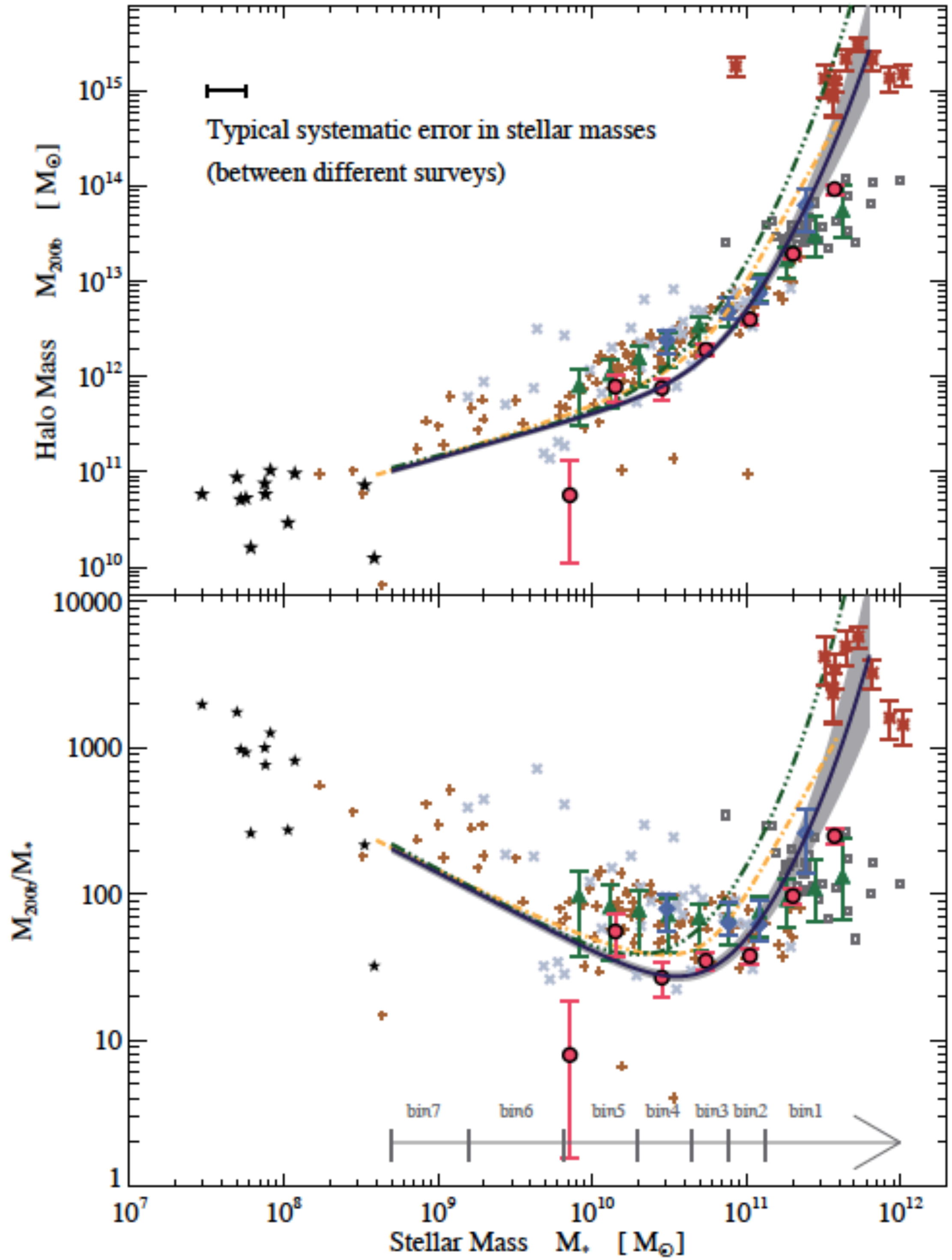

Typical systematic error in stellar masses
(between different surveys)
Halo Mass $M_{200b}$ [$M_\odot$]
$M_{200b}/M_*$
bin7
bin6
bin5
bin4
bin3
bin2
bin1
Stellar Mass $M_*$ [$M_\odot$]

# モデル詳細

全てのモデルで、SFRを$M_h$, zの関数としてモデル化
->SHMRを計算

1. ガス冷却モデル

$$\mathrm{SFR} = \epsilon_{\mathrm{SF}} \frac{M_{\mathrm{gas}}}{t_{\mathrm{cool}}}, \quad M_{\mathrm{gas}} = f_{\mathrm{gas}} f_{\mathrm{b}} M_{\mathrm{h}}, \quad t_{\mathrm{cool}} = \frac{E_{\mathrm{k}}}{|\dot{E}_{\mathrm{cool}}|} = \frac{3}{2} \frac{k_{\mathrm{B}} T}{n \Lambda(T)}$$

2. Negative feedbackモデル

$$\log\left[\frac{SFR}{\mathrm{M_\odot\ yr^{-1}}}\right] = (1.25 \pm 0.03) + (0.81 \pm 0.04) \log\left[\frac{M_*}{10^{10}\ \mathrm{M_\odot}}\right]$$

$$\eta \propto M_{\mathrm{dyn}}^{-0.4}$$

# モデル詳細

3. Positive feedbackモデル

$$SFR = \epsilon_{\mathrm{pf}} \frac{M_{\mathrm{gas}}}{t_{\mathrm{dyn}}} \quad t_{\mathrm{dyn}} = \frac{r_{\mathrm{disk}}}{\sigma} \quad \frac{1}{2}\rho\sigma^2 = \frac{1}{2} n m_{\mathrm{p}} \mu \sigma^2 = P$$

4. Merger/accretionモデル

$$SFR = F_{\mathrm{dry}} SFR_{\mathrm{dry}} + F_{\mathrm{wet}} SFR_{\mathrm{wet}} + F_{\mathrm{mix}} SFR_{\mathrm{mix}},$$

$$SFR_{\mathrm{dry}} = SHMR(M_{\mathrm{h}}, z) \frac{dM_{\mathrm{h}}}{dt}(M_{\mathrm{h}}, z)$$

$$SFR_{\mathrm{wet}} = \frac{-M_* + M_{*,\mathrm{wet}}}{\Delta t} = \frac{-M_* + f_{\mathrm{b}} M_{\mathrm{h}}}{\Delta t}$$

$$SFR_{\mathrm{mix}} = f_{\mathrm{b}} \frac{dM_{\mathrm{h}}}{dt}(M_{\mathrm{h}}, z).$$

# すばる/HSC 測光カタログ

- 測光カタログは、hscPipeで作られている
- hscPipeによる測光 ≠ 過去の研究
  - z~5銀河の面密度が合わない
  - 本研究では、自身で測光カタログを作成

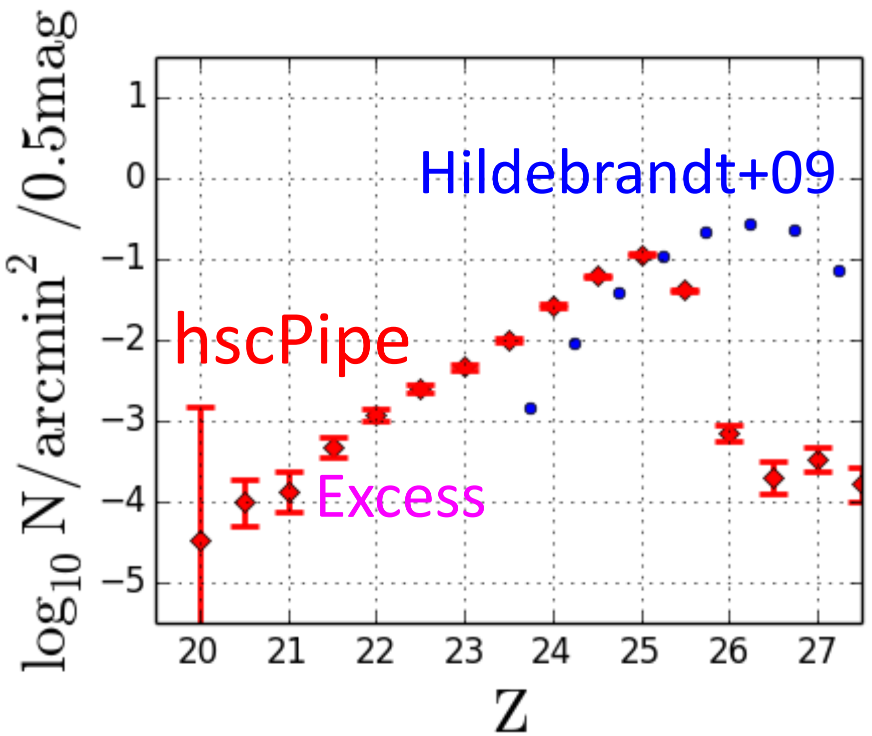


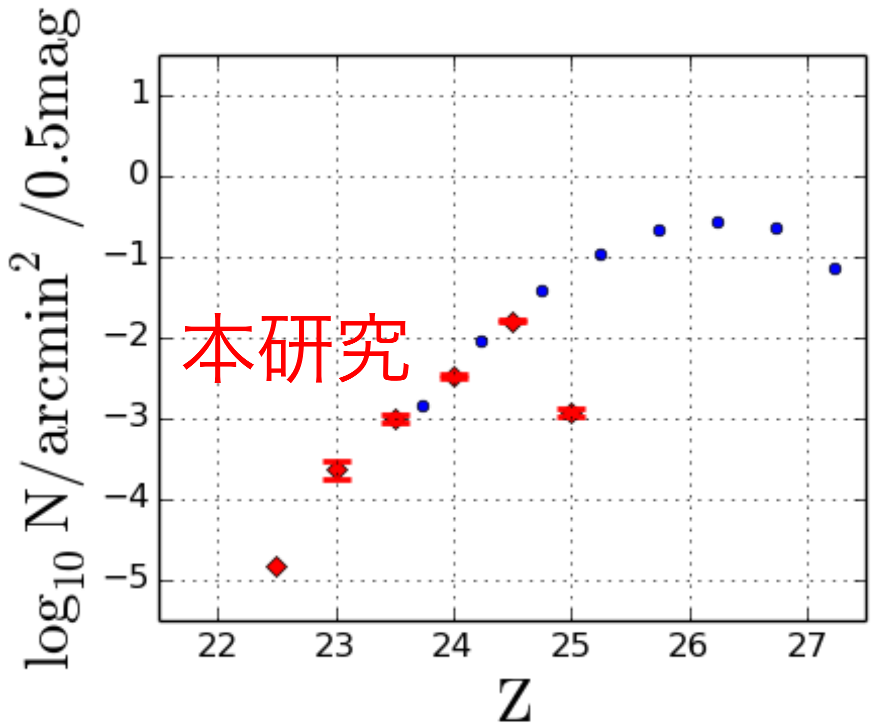

# すばる/HSC 測光カタログ

- ID=37480289806603784

tract = 8522
patch = 7,7
z(cmodel) = 22.4

- ID=37481144505094658

tract = 8522
patch = 1,0
z(cmodel) = 22.8

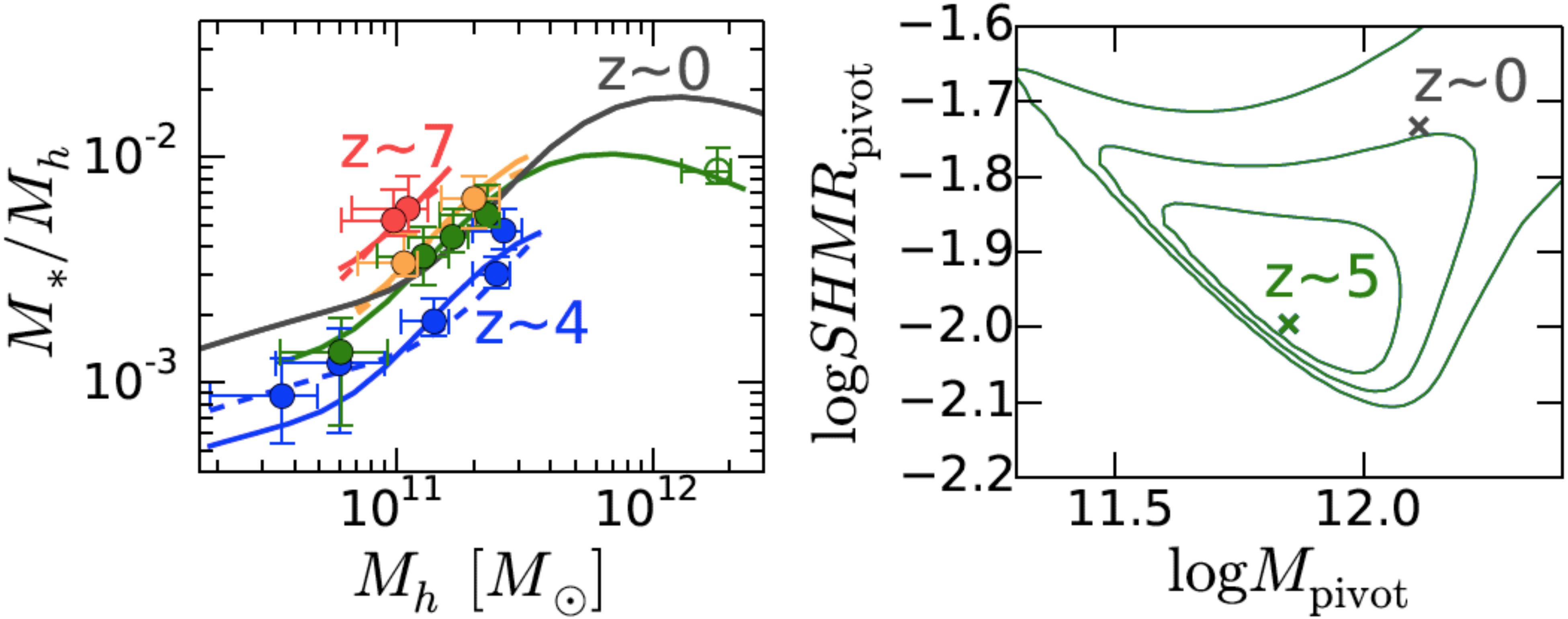

z~0
z~7
z~4
$10^{-2}$
$10^{-3}$
$M_*/M_h$
$10^{11}$
$10^{12}$
$M_h\ [M_\odot]$
−1.6
−1.7
−1.8
−1.9
−2.0
−2.1
−2.2
z~0
z~5
11.5
12.0
$\log SHMR_{\rm pivot}$
$\log M_{\rm pivot}$

# Baryon Conversion Efficiency (BCE)

- BCE =SFR/(d$M_b$/dt)
  - バリオンガス->星への変換効率
  - d$M_b$/dt=$f_b$ x d$M_h$/dt(z,$M_h$) ($f_b$=$\Omega_b$/$\Omega_m$)

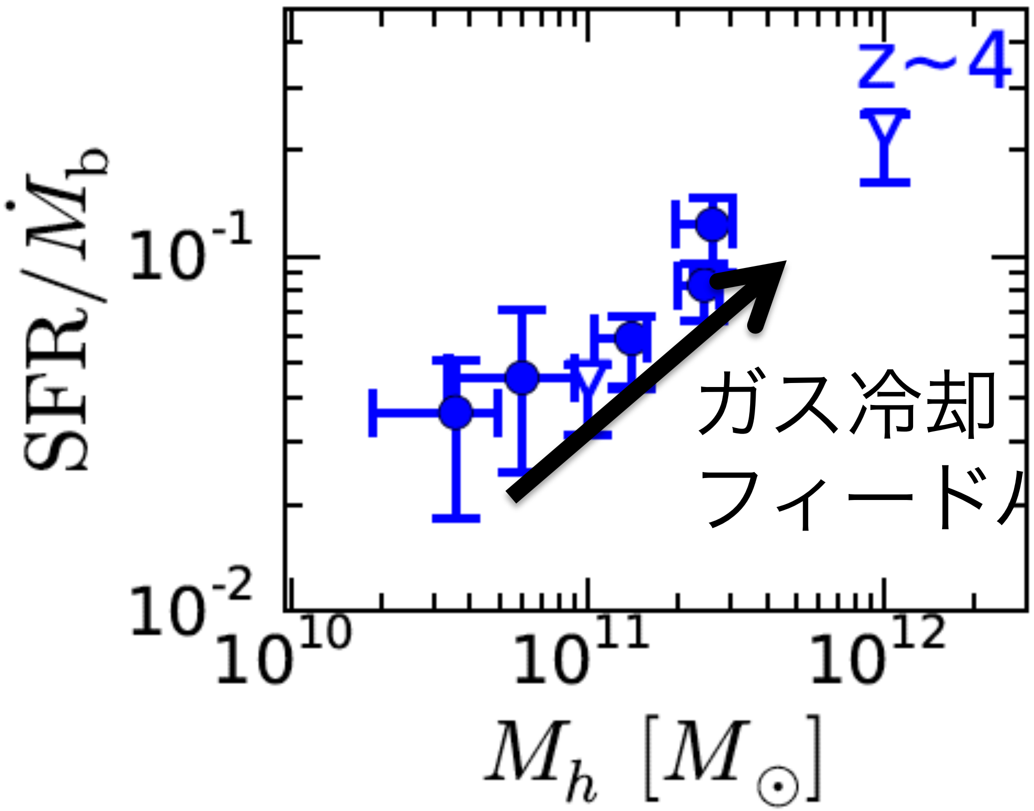


●z~4
▽z~4
(Behroozi+13)

# SHMR($M_h \sim 10^{11}\ M_{sun}$)進化の予想

シミュレーション (理論)

z~6->z~0で単調増加

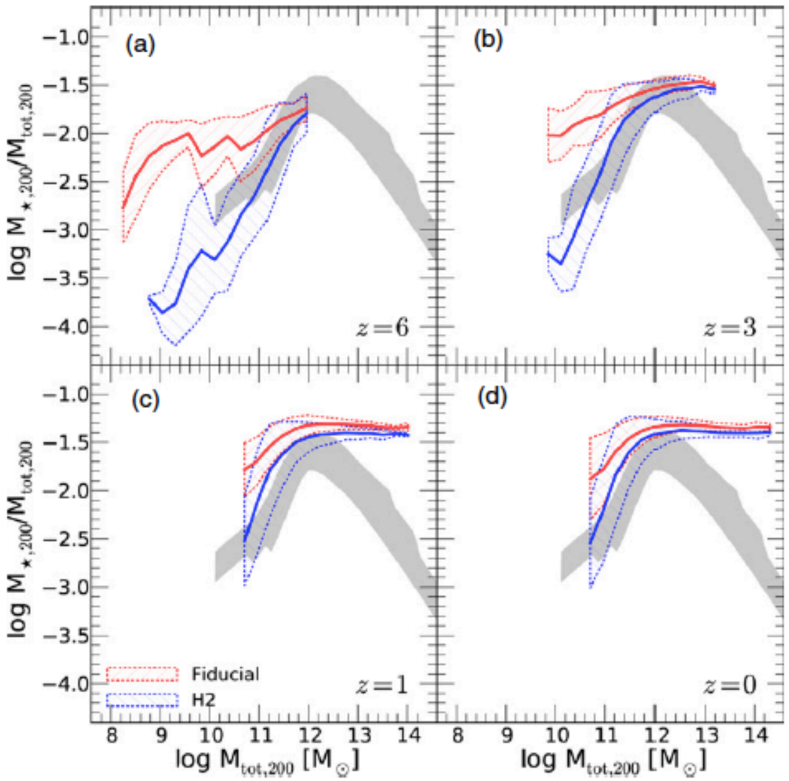

Thompson+14

アバンダンスマッチング (観測+モデル)

z~8->z~2で減少

z~2->z~0で増加

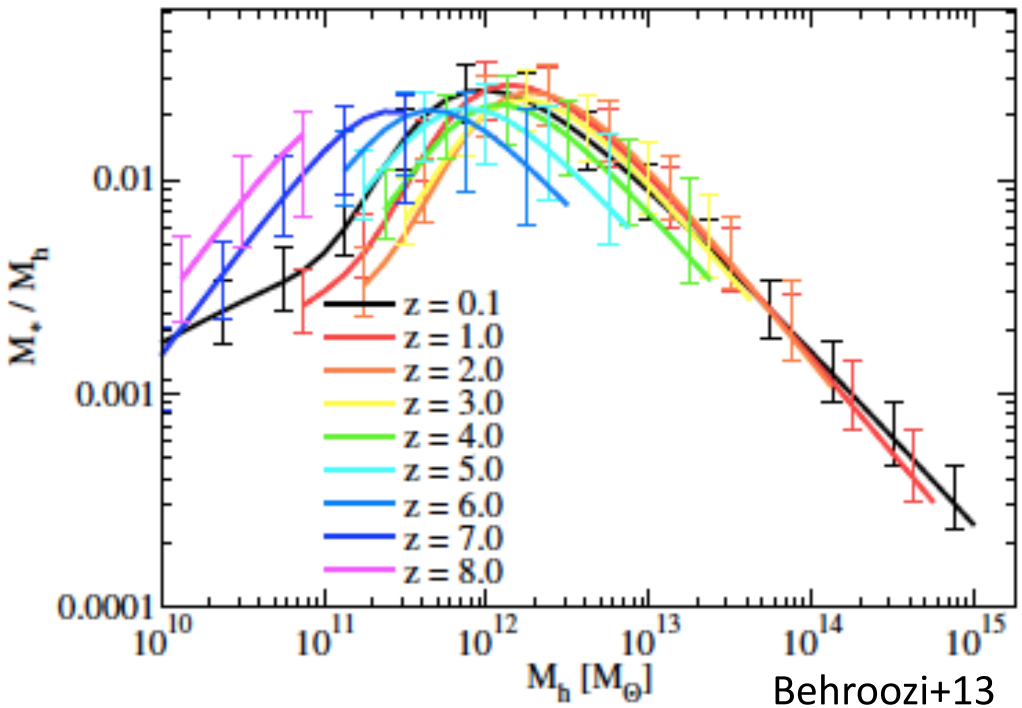

Behroozi+13